6-29-2010

Synthesis, Characterization, and Self-Assembly of Gold Nanorods and Nanoprisms

Kristina L. Tran
University of South Florida

Synthesis, Characterization, and Self-Assembly of Gold Nanorods and Nanoprisms

by

Kristina L. Tran

A thesis submitted in partial fulfillment
of the requirements for the degree of
Master of Science in Chemical Engineering
Department of Chemical & Biomedical Engineering
College of Engineering
University of South Florida

Major Professor: Vinay Gupta, Ph.D.
Kirpal Bisht, Ph.D.
Norma Alcantar, Ph.D.

Date of Approval:
June 29, 2010

Keywords: resorcinarenes, macrocycles, anisotropic gold nanoparticles, metal nanoparticles, binary surfactant synthesis

Table of Contents

List of Tables

List of Figures

Synthesis, Characterization, and Self-Assembly of

Gold Nanorods and Nanoprisms

Kristina L. Tran

Abstract

The unique properties of gold nanoparticles make them excellent candidates for applications in electronics, sensing, imaging, and photothermal therapy. Though abundant literature exists for isotropic gold nanoparticles, work on nanoparticles of different shapes has been gaining interest recently. Anisotropic gold nanoparticles, such as nanorods and nanoprisms, have tunable optical properties in the visible and near-infrared regions. Through synthesis and surface modification, the production of various shapes of these gold nanoparticles can be controlled to meet different applications.

Two different types of gold nanorods were used in this thesis. The first type was stabilized with cetyltrimethylammonium bromide (CTAB) and had aspect ratios of 3-4 (defined as the nanorod length divided by the diameter). The second type was synthesized using CTAB and benzyldimethylhexadecylammonium chloride (BDAC) in a binary surfactant system which produced aspect ratios greater than 4. The nanorods were characterized with UV-Vis spectroscopy and transmission electron microscopy (TEM).

Two types of bowl-shaped macrocyclic compounds called resorcinarenes were used to direct self-assembly of the nanorods. The first type of resorcinarene (R2S) consisted of thiol(SH)-terminated alkyl chains on both rims. The second type (R1S) contained thiol-terminated alkyl chains on only one rim. The monolayer formation of these resorcinarenes on planar gold surfaces was studied and characterized by FTIR spectroscopy. Resorcinarene-mediated assembly of gold nanorods was monitored with UV-Vis spectroscopy, dynamic light scattering (DLS), and TEM. In addition to gold nanorods, gold nanoprisms were synthesized through a kinetically-controlled reduction route in the presence of CTAB. The linking of nanoprisms using resorcinarenes was also explored.

Chapter 1:

Introduction, Motivation, and Background

For decades, metal nanoparticles (1-100 nm in size) have been of particular research interest due to their unique optical and electronic properties, which make them attractive for a variety of applications. On a nanoscale, metallic particles exhibit properties that differ from bulk properties due to the surface confinement of electrons[1]. For example, the surface plasmon resonance (SPR) of these nanoparticles is widely studied due to its ease of characterization and coupling with electronic and magnetic properties. Plasmon absorptions of nanoparticles can be tunable due to size and morphology[2]. Through careful control of experimental parameters, different nanoparticle shapes can be produced.

In addition to the synthesis of these nanoparticles, the two- and three-dimensional assembly of these materials becomes an increasingly vital facet of the field of nanoscience. The controlled self-assembly of nanoparticles can provide benefits in electronics, sensing, and catalysis[3].

The aims of this thesis are twofold: one, to control surfactant-mediated synthesis of gold nanorods and nanoprisms and second, to examine the particle-particle interactions in their self-assembly with a class of macrocyclic compounds called resorcinarenes.

The following sections will briefly describe the background on isotropic gold nanoparticles and the growing research on anisotropic gold nanoparticles. A brief literature review of surface modification of these nanoparticles for self-assembly will also be discussed.

1.1. Isotropic Gold Nanoparticles

Gold nanoparticles are known to have strong absorption in the UV-visible range. Solution synthesis of isotropic gold nanoparticles is performed in a number of ways. One common route is the reduction of $HAuCl_4$ to gold ions. First used by Turkevitch in the early 1950s to produce gold nanospheres using sodium citrate as a reducing agent[4,5], the reduction method has been adapted by numerous researchers to synthesize nanoparticles of various sizes[5]. It was initially used to synthesize isotropic nanoparticles approximately 15 nm in diameter, the procedure involves the reaction[4-5]:

$$6AuCl_4^- + C_6H_8O_7 + 5H_2O \rightarrow 6CO_2 + 24Cl^- + 6Au^0 + 18H^+$$

Researchers thereafter have produced nanoparticles of various sizes up to 150 nm by changing various experimental parameters such as type and concentration of reducing agent[2, 5].

The seed-mediated growth method has also been employed by many groups. In this process, gold seeds are formed first. Then a weak reducing agent such as ascorbic acid is introduced into the solution to reduce the gold ions onto

the surface of the seeds[2]. Murphy and colleagues have found that they could make gold nanospheres of controllable sizes by adjusting the seed-to-precursor ratio[5-6].

The unique optical properties of gold nanoparticles can be attributed to the principles of light scattering. In 1908, Gustav Mie developed a model that described the absorption and scattering extinction of spherical particles by solving Maxwell's equations[7] . Because it can be applied to particles of any size, Mie's theory has been popular for solutions containing isotropic nanoparticles[5].

The interaction of an electromagnetic field with metallic conduction band electrons produces localized oscillations of the electron clouds. Figure 1.1a illustrates the behavior of surface plasmon oscillation in a spherical gold nanoparticle. Under the electric field of an incident light wave, the free electrons are displaced from the positive core. The charge difference produces a dipolar oscillation at a resonant frequency of the conduction electrons[8].

When electrons are confined to the surface, the localized surface plasmons contribute to the increase of field enhancement at the nanoparticle surface. This phenomenon in resonance leads to an amplification of the field in the visible range of the electromagnetic spectrum. The surface plasmon resonance is a function of a number of features, namely particle size, morphology, dielectric medium, particle interactions, and local chemical environment. Thus, for 20 nm diameter nanospheres in an aqueous solution, a strong absorption peak is seen in this region at around 520 nm, which accounts for both the scattering and absorption[9]. The scattering process consists of the

release of photons during the nanoparticle's absorption of the incident light at this resonant frequency. The simultaneous absorption takes place during the conversion of some photons into phonons (lattice vibrations). The SPR peak results in a bright red solution color of the gold nanoparticles, which renders them useful for optical applications[8-10].

In recent years, the seed-mediated growth method for nanoparticles popularized by Jana, Murphy, and others has also seen success in fabricating nanoparticles of controlled sizes. In this technique, a strong reducing agent such as sodium borohydride can be used to reduce Au^{3+} ions to gold seeds. When a weak reducing agent is introduced to the solution, Au^{3+} ions would be reduced onto the surface of the existing seeds[2]. It was shown that the morphology and size of these nanoparticles can be controlled by varying the reaction conditions.

1.2. Anisotropic Gold Nanoparticles

Of recent interest is the use of non-spherical or anisotropic gold nanoparticles in biomedical, optical, and sensing applications. The properties that govern their use in these applications are the plasmon absorption and the increased surface-enhanced Raman scattering due to shape modification of gold nanoparticles. The latter is due to the plasmon band of the gold surface coupling with that of the adsorbed species[10]. Given the potential applications, it becomes important to control the physical parameters of the gold nanoparticles, such as size and shape, in order to manipulate their optical and electronic properties. Shape control provides tuning over a wider range in the electromagnetic

spectrum than isotropic nanoparticles. Anisotropic gold nanoparticles can absorb in the near-infrared range, which makes them valuable as photothermal agents for biological applications where, coupled with the known biocompatibility of gold, absorption by tissues in this region is minimal[11].

Proven methods of altering the shapes of gold nanoparticles include varying the concentrations of surfactants and reducing agents, as well as kinetically controlling reaction conditions[12]. Some of the unusual shapes that have resulted from these modifications include rods, prisms, cubes, pyramids, wires, and polyhedras[13]. This thesis will focus on gold nanorods and gold nanoprisms.

1.2.1. Gold Nanorods

Out of the anisotropic gold nanostructures, nanorods have been receiving a lot of attention for their optical properties and applications. Because Mie's theory only applies to isotropic particles, it cannot be used to model the optical behavior of nanorods. In 1912, Richard Gans modified the boundary conditions in Mie's theory for spheroids to predict the existence of two absorption bands[7]: a transverse band associated with the width of the rod and a longitudinal band related to the length of the rod[5]. As illustrated in Figure 1.2, the transverse band has a peak around 520 nm, and the longitudinal band can be adjusted towards the near-infrared region by increasing the aspect ratio of the nanorod[14]. For nanorods, the electric field across the particle is not uniform as observed for

isotropic nanoparticles so the multipolar excitations result in more than one peak in the spectra[8].

The crystallography of gold nanorods has been well-published. Figure 1.3 is a schematic of a typical gold nanorod. The end facets are {111}, while the longitudinal axis is {110}[10]. It is the {110} surface that is speculated to be a preferential binding site for the CTAB bilayer, forcing anisotropic growth on the {111} ends[15].

By controlling the synthesis conditions, nanorods of different aspect ratios can be produced[10,11]. Over the years, various protocols have been developed to produce gold nanorods. This includes porous aluminum template, electrochemical, photochemical, and seed-mediated growth methods[16]. The latter has been widely adopted in synthesizing higher aspect ratio nanorods.

In a typical seed-mediated growth synthesis, a seed solution is prepared by reduction of $HAuCl_4$ in the presence of a surfactant such as cetyltrimethylammonium bromide (CTAB) with cold sodium borohydride. A growth solution consisting of $HAuCl_4$ reduced by ascorbic acid, silver nitrate, and CTAB. Addition of the seed solution to the growth solution provides nucleation sites for growing nanorods. The mechanism has yet to be fully elucidated, but one well-known hypothesis is that the surfactant is used as a stabilizer as well as a capping agent to preferentially attach to the {100} facets of the seeds. This acts to retard growth in that direction and to permit elongation on the {111} facets at the ends of the rods[1, 17].

Nikoobakht and El-Sayed adopted the seed-mediated growth protocol to include a co-surfactant benzyldimethylhexadecylammonium chloride (BDAC) to increase the aspect ratio. Through variation of the ratio of the two surfactants and the silver nitrate concentrations, they were able to synthesize gold nanorods of aspect ratio of ten[15].

Researchers have also found that a variety of nanostructures could be produced by using a surfactant as a shape controller to direct nanoparticle growth[13b, 18]. Huang and colleagues have shown that by simply by changing the CTAB concentration through a hydrothermal route, they were able to synthesize various structures (polyhedral, nanoprisms, hexagonal nanoplates) in high yield. In addition to its role as a nanoparticle stabilizer and shape director, CTAB decomposes under hydrothermal conditions to promote reduction of Au^{3+} to Au^{0}, which aids in forming different nanostructures for different amounts of CTAB[13b].

Sau and Murphy adjusted different experimental parameters to the seed-mediated growth protocol to develop gold nanoparticles of different shapes such as cubes, tetrapods, triangles, and branched particles. They systematically varied the concentrations of CTAB, ascorbic acid, gold seed, gold ions, and silver nitrate to produce high yields (most over 70%) of different morphologies[18].

1.2.2. Gold Nanoprisms

Though nanorods have been one of the most widely studied amongst anisotropic gold nanoparticles for a long time, attention has been given to other types of gold nanomaterials recently. Triangular nanoprisms are two parallel

triangle faces of a certain thickness between them. This thickness can be up to 50 nm, while the edge length can vary from 40 nm to micrometer sized[19].

Typically, gold nanoprisms prepared in solution have {111} facets on the triangular faces, while the edges are either {110}, {111}, or {100} (see Figure 1.4). The aspect ratio (edge length divided by thickness) usually ranges from 5 to 40[19].

As with gold nanorods, nanoprisms also exhibit tunable SPRs in the visible and near-infrared regions due to variations in length, thickness, dielectric medium, and tip shape. In contrast to a dipole plasmon mode seen in gold nanorods, high aspect ratio nanoprisms (greater than 10) have a quadropole plasmon mode. Millstone and co-workers monitored the synthesis of gold nanoprisms over time using UV-Vis-NIR spectroscopy and found their results comparable to discrete dipole approximation calculations[19].

There are two main synthetic routes frequently used to synthesize gold nanoprisms: photochemical and thermal syntheses. The earlier method is the photochemical procedure first used to produce silver nanoprisms. Mirkin and others have demonstrated the conversion of silver nanoparticles to triangular nanoprisms by fluorescent irradiation. They also found that adjusting the excitation wavelength gave control over the edge length[19]. Similarly, Takezaki and co-workers obtained high-yield results for gold nanoprisms after they used a mercury lamp to irradiate a gold/surfactant solution for three hours[20]. Another method of yielding nanoprisms in solution is through a kinetically-controlled chemical reduction route. In solution, a chemical reduction of a gold precursor

with a surfactant yields gold seeds that grow into nanoprisms in high reaction temperatures[21].

1.3. Self-Assembly of Nanoparticles through Surface Modification

It is important to not only understand the synthesis, structure, and properties of nanomaterials but also to be able to manipulate how they interact with each other. The self-organization of nanoparticles has been a hotly researched area over the past decade. As protocols of nanoparticle synthesis are continuously being refined, it becomes increasingly important to study how they can be exploited to self-assemble for applications such as nanodevices.

Self-assembly using molecular ligands requires attention to the surface chemistry and interaction of the nanoparticles. Existing approaches for assembling gold nanorods include those governed by biotin/streptavidin linking[22], intermolecular hydrogen bonds[23], electrostatic forces[24], and dithiol molecules[25].

One well-known mode of nanorod linkage pioneered by Murphy and colleagues in 2003 takes advantage of the strong biotin-streptavidin bond. Gold nanorods were surface-functionalized with biotin. Upon the introduction of streptavidin to the nanorods, it was found that end-to-end chaining occurred in high percentages[22].

Hu and others showed that self-assembly of gold nanorods could also be done by using cysteine as a molecular linker. They showed that the nanorods functionalized with the terminal thiol group in cysteine displayed end-to-end assembly through intermolecular hydrogen bonding between the amino acids.

Upon nanorod linking, a red-shift in the longitudinal absorption peak was noticed, coinciding with the plasmonic coupling of the nanorods in contact with each other[23].

Another way of assembling gold nanorods does not require covalent modification of the surface. Rather, it depends on the surface charges of the nanorods for electrostatic interactions. Demonstrated by Park and co-workers, both side-to-side and end-to-end assembly was done with disodium chromoglycate. Under a positively-charged environment, the CTAB-coated nanorods are assembled laterally with the negatively-charged disodium chromoglycate. For a negative surface charge on the nanorods, they introduced poly(acrylic acid) to the medium. The new surface coating left the end faces of the rods free to attract the disodium chromoglycate for end-to-end organization[24].

Dithiol linkers are a straightforward way of inducing self-assembly in gold nanoparticles. By taking advantage of the strong gold-thiol bond, Joseph and others used alkanedithiols to join together nanorods in an end-to-end fashion. Through time studies, these researchers proposed that nanorod linking occurred in two steps. The first step, termed the incubation step, sees no optical changes, suggesting that the nanorods are segregated and that one side of the dithiol molecule is attached to a {111} end of the nanorod. Following this stage, the free thiol ends come into contact with nearby nanorods. Similar to what others have reported, the nanorods chain up, plasmon coupling occurs and is reflected in the red-shifts in the absorption spectrum[25].

Presented so far are only a few ways out of the many that are used to investigate the self-assembly of gold nanoparticles. For this thesis, a unique class of macrocyclic compounds called resorcinarenes was chosen to mediate nanoparticle self-assembly.

1.4. Resorcinarenes

Resorcinarenes (or calix[4]arenes) are a group of bowl-shaped macrocycles synthesized from the condensation of resorcinol with an aldehyde (see Figure 1.5). The bowl-shaped confirmation of these compounds refers to its upper rim being wider than the lower rim, either of which can be substituted with different functional groups[26]. In addition to having a bowl or “crown” confirmation, they can adopt other stereochemical configurations such as boat and chair[27]. These molecules have received a lot of attention in supramolecular chemistry due to self-assembly in solution to produce large cavities that can include or “host” smaller molecules for guest-host interactions[28].

Their role in the field of metal nanoparticles is one that is garnering great interest recently. For instance, Kim and co-workers have coated gold nanoparticles with resorcinarenes and have used them for self-assembly and extraction at liquid interfaces. They also observed a high degree of order when the encapsulated nanoparticles self-assembled into arrays[29].

For the resorcinarenes used in this research, the multiple thiol groups have been built to offer advantages of stronger linking and multiple sites for self-

assembly of the gold nanostructures. More details about these self-assembly effects and the characterization will be discussed in subsequent chapters.

1.5. Thesis Organization

This thesis is organized as follows. Chapter 2 describes the synthesis of gold nanorods using a two-surfactant system of CTAB and BDAC. Chapter 3 is devoted to the investigation of resorcinarene-mediated self-assembly of two types of gold nanorods: one coated with CTAB alone and the other coated with both CTAB and BDAC. In Chapter 4, the synthesis and self-assembly of CTAB-stabilized gold nanoprisms is investigated as an extension of this research on anisotropic gold nanomaterials. Finally, Chapter 5 recapitulates the work done in this thesis.

(a)

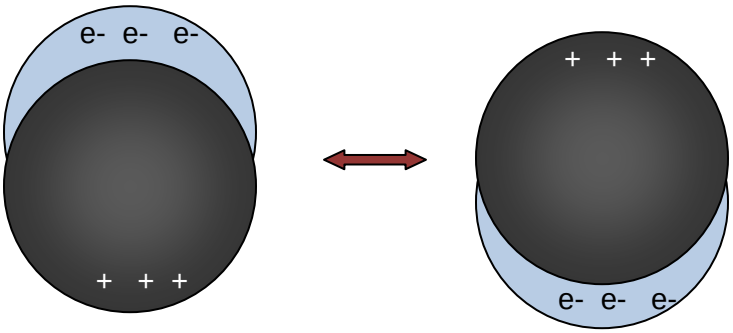

(b)

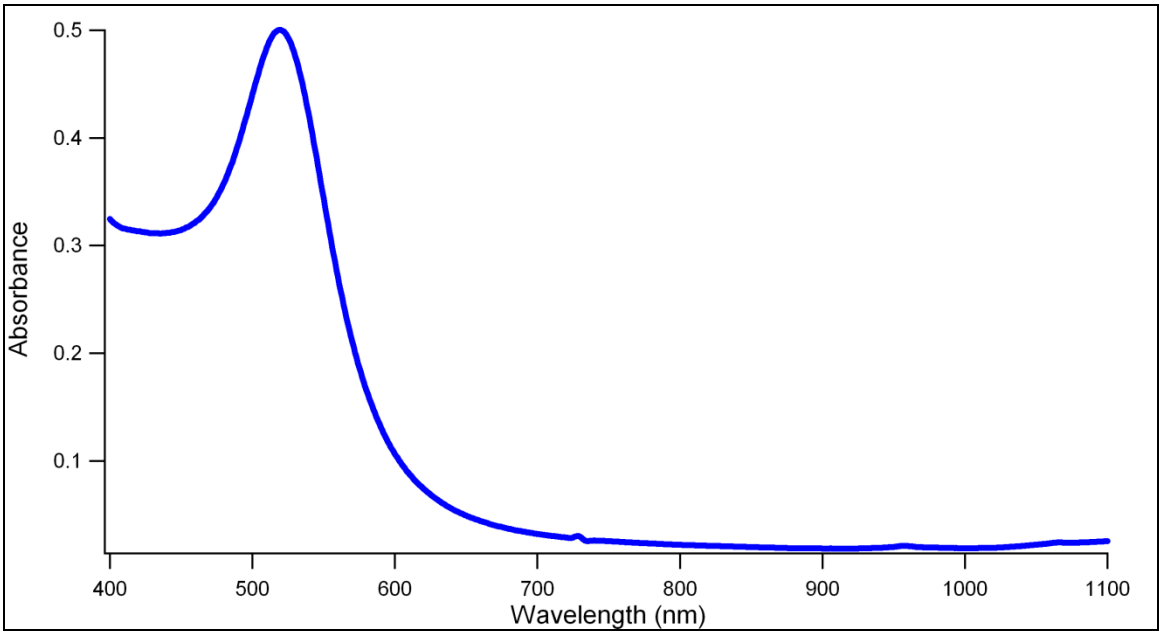

Figure 1.1. (a) Schematic of surface plasmon oscillation for an isotropic gold nanoparticle (b) A typical absorption spectrum of an aqueous solution of gold nanoparticles in a dispersed state.

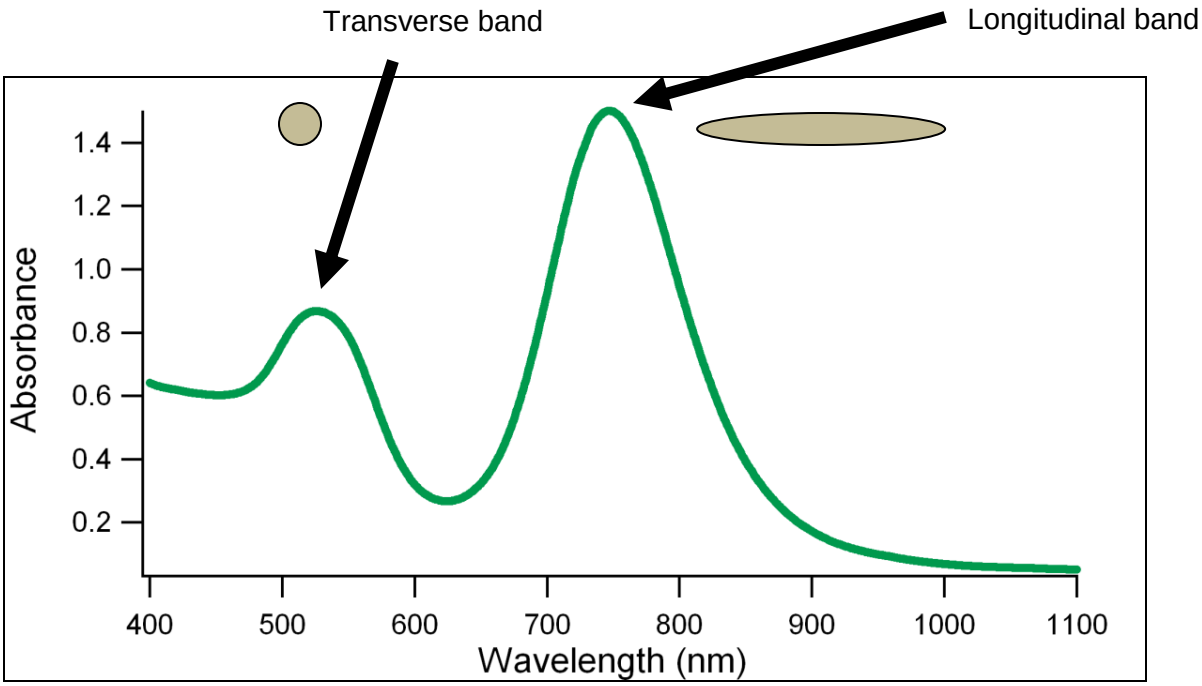

Figure 1.2. Typical absorption spectrum of an aqueous solution of gold nanorods in a dispersed state.

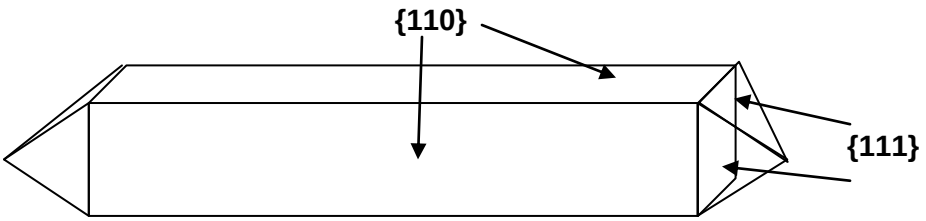

Figure 1.3. Schematic crystallography of gold nanorods with ends dominantly {111} crystallographic planes and the side facets dominantly {110}. These rods are typically formed using seed-mediated approaches. Adapted from Murphy et al., *Journal of Physical Chemistry B*, 2005, 109(29): 13857-13870.

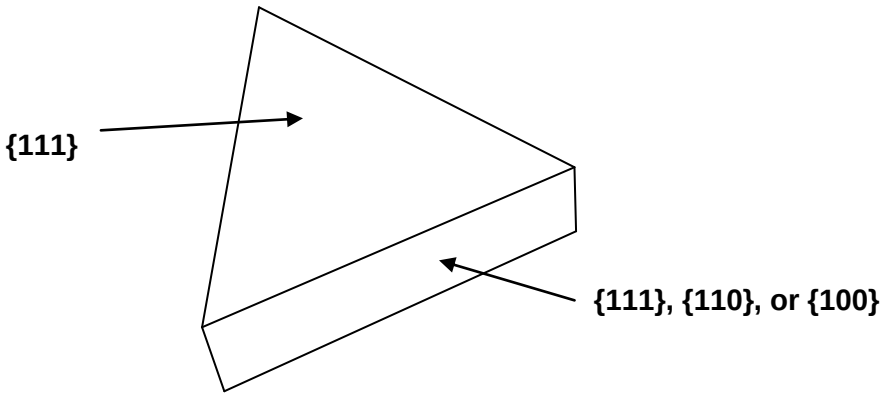

Figure 1.4. Schematic of the crystallography of a gold nanoprism. The top and bottom surfaces are {111} and the side facets are {110}, {100}, or {111}. Adapted from Millstone et al., *Small*, 2009, 5(6): 646-664.

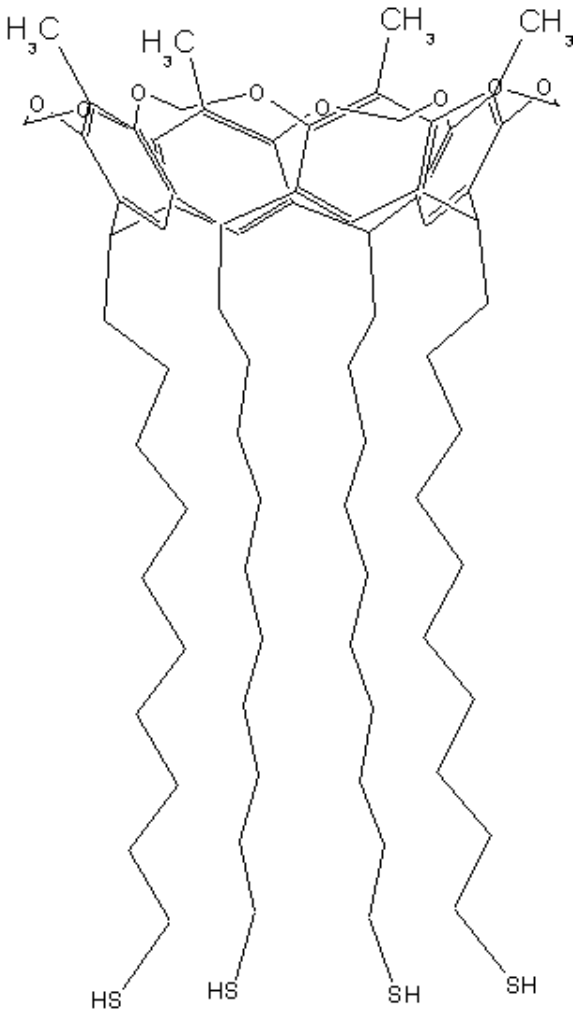

Figure 1.5. Schematic illustration of a resorcinarene with thiol-terminated alkyl chains on the lower rim. These macrocyclic compounds can be tailored to add different functional groups.

Chapter 2:

Controlled Synthesis of Gold Nanorods Using a Binary Surfactant System

2.1. Enhancements in the Aspect Ratio of Gold Nanorods

Two types of gold nanorods were employed for self-assembly studies in this thesis: one type included nanorods that have aspect ratios less than 3 stabilized with only one surfactant (cetyltrimethylammonium bromide or CTAB); these were synthesized by Walker in our laboratory[30]. The second type of nanorods had aspect ratios greater than 3 and were stabilized with two surfactants (CTAB and benzyldimethylhexadecylammonium chloride or BDAC). The synthesis of this system was investigated as a function of experimental parameters (surfactant concentrations, additives such as silver nitrate, etc.) in order to look at the effects of nanorod aspect ratio on the quality of linear self-assembly. Additionally, size separation of the gold nanorods using centrifugation was investigated in an attempt to minimize the amount of isotropic particles in solution.

Using a modification of Sharma and co-workers' synthesis of gold nanorods with binary surfactant system[31], a gradual addition of ascorbic acid to the growth solution, as well as variation of experimental parameters, was also used to increase and optimize the aspect ratio of the gold nanorods.

The mechanism of gold nanorod formation with CTAB and BDAC has yet to be fully understood, but researchers speculate that the surfactants and silver

ions promote anisotopic growth along the longitudinal direction through the selective binding of the {110} facet on gold[15, 31]. It is reported that the CTAB/BDAC surfactant system boasts a lower critical micelle concentration than a singular CTAB system. This could lead to a better formation of micelles in solution, which binds to the gold salt to slow its reduction and also functions to face block the nanorods to force elongated growth. The role of the silver ions is speculated to be collaborating with the CTAB to facilitate packing and attachment to the gold nanorod surface[15, 31].

2.1.1. Experimental

2.1.1.1. Materials

CTAB and BDAC were obtained from TCI America. Sodium borohydride and silver nitrate were purchased from Acros Organic. Gold (III) chloride trihydrate was purchased from Sigma Aldrich. L-ascorbic acid was obtained from Fisher Scientific. Water used for all synthesis is from EasyPure UV System (from Barnstead, IA), where particulate matter was removed via a 0.2 μm filter.

2.1.1.2. Synthesis of Gold Nanorods Stabilized with Two Surfactants: Gradual Addition of Ascorbic Acid

Aqueous stock solutions containing 0.25 M CTAB and 0.25 M BDAC were prepared separately and heated to 35°C before each synthesis. A seed solution containing CTAB and $HAuCl_4$ in water was made. Enough ice cold sodium borohydride was added to the seed solution until it turned brown, indicating gold

seed formation. The seed solution was then left to stir in the hood for one hour at room temperature so that the reduction goes to completion.

The growth solution was prepared with a CTAB/BDAC ratio of 0.67. Then 0.01 M $HAuCl_4$, 0.01 M $AgNO_3$, and 0.01 M ascorbic acid were added to the growth solution in that order. Quantities of the solutions followed the published procedures in literature[31]. After mixing by inversion, UV-Vis and DLS measurements were taken for t=0 before a small amount (10-50 µL) of diluted seed was added to each growth solution.

The UV-Vis spectra and DLS were taken every few hours, and the DLS was programmed to take readings every hour while the experiment was left overnight. When it was determined the nanorods have stopped growing based on no further changes in the UV-Vis spectra, small amounts of 0.01 M ascorbic acid were added to the growth solution to reinitiate growth, which was monitored through UV-Vis spectroscopy and DLS. When the absorption spectra appeared to stop red-shifting, more ascorbic acid was introduced to the nanorod growth solution. Purification of the nanorods is described in detail later.

2.1.1.3. Synthesis of Gold Nanorods Stabilized with Two Surfactants: Variation of Silver Nitrate Concentration

Aqueous stock solutions containing 0.25 M CTAB and 0.25 M BDAC were prepared separately and heated to 35°C before each synthesis. A seed solution containing CTAB and $HAuCl_4$ in water was made. Enough ice cold sodium borohydride was added to the seed solution until it turned brown, indicating gold

seed formation. The seed solution was then left to stir in the hood for one hour at room temperature so that the reduction goes to completion.

The growth solution was prepared with a BDAC/CTAB ratio of 0.67 as before. Then 0.01 M $HAuCl_4$, 0.01 M $AgNO_3$ (varied from 1.6-2.2% of total solution volume), and 0.01 M ascorbic acid were added to the growth solution in that order. After mixing by inversion, UV-Vis and DLS measurements were taken for t=0 before seed solution was added to each growth solution. Gradual addition of either ascorbic acid or a separate growth solution was introduced to the nanorod solution in an attempt to increase the aspect ratio. UV-Vis spectroscopy and DLS was used to monitor the growth of the nanorods. Purification of the nanorods is described in detail in the next section.

2.1.2. Results and Discussion

Figure 2.1 shows a typical UV-Vis spectrum of CTAB-stabilized nanorods where the longitudinal peak is around 750 nm. A typical DLS size distribution of these nanorods is shown in Figure 2.2. TEM images in Figure 2.3 show the short aspect ratio of the nanorods synthesized with CTAB.

Figure 2.4 shows a typical DLS size distribution of the nanorods stabilized with CTAB and BDAC. In Figure 2.5, the UV-Vis spectra are given for gold nanorods synthesized in a co-surfactant system with the stepwise addition of ascorbic acid. With the initial addition of 600 µL of ascorbic acid, the longitudinal peak red-shifted gradually to about 858 nm within the first 18 hours. Afterwards, 100 µL of ascorbic acid was added to the growth solution to further red-shift the

peak. This resulted in a peak intensification and a shift to 869 nm. After 24 hours from the initial time, two more additions of 50 µL of ascorbic acid were done. This resulted in very small changes in the peak shift.

The DLS trend graph of nanorod size for Peak 2 from Figure 2.4 over time is shown in Figure 2.6. It shows the first stage of nanorod growth leveling off after nine hours. As more ascorbic acid is added to the solution, the particle size increases. The multiple additions of ascorbic acid serve to better control the reduction rate of the gold ions in order to slowly grow the gold nanorods to a longer length. The first stage of growth established the general width of the nanorods with the use of the surfactants. Each additional ascorbic acid reduction step provided more gold to deposit more at the ends of the existing nanorods while maintaining its initial diameter. The potential for tuning to a desired length is open; however, too much ascorbic acid can blue shift the absorption spectra as the nanorod begins to grow thicker instead of longer due to the increased gold supply[31].

To further increase the aspect ratio of the rods, another experimental parameter was explored: silver nitrate concentration. Figure 2.7 illustrates how increasing the silver content affects the aspect ratio of the nanorods. The highest amount of $AgNO_3$ tested showed a decrease in the aspect ratio, and this observed trend agrees with literature[15].

2.2. Shape Separation of Gold Nanorods

In nanorod synthesis, monodispersity remains a challenge in colloidal science. There will often be isotropic structures formed when synthesizing gold nanorods, hence, purification is important[32]. Existing methods of separating nanoparticles include electrophoresis and chromatography[3]. The separation method that was employed in this research was centrifugation. According to Sharma and colleagues who carefully studied the theoretical sedimentation for rods and spheres, a key parameter for shape separation is the diameters to the second power of the particles[31].

The rod-to-sphere sedimentation ratio for nanoparticles in Brownian motion during centrifugation is calculated by Sharma and others to be

$$\frac{s_o^{rod}}{s_o^{sphere}} = 6\left(\frac{D}{2a}\right)^2\left[2ln\left(\frac{L}{D}\right) - (v_\perp + v_\parallel)\right]$$

where D is the diameter of the particle, a is the radius of the sphere, L is the length of the particle, and $(v_\perp + v_\parallel)$ are correction factors accounting for the perpendicular and parallel orientation of the rods[31]. It can be seen that the aspect ratio (L/D) is not as influential as the diameters of the nanoparticles. This suggests that nanoparticles with smaller diameters sediment slower than those with larger diameters.

2.2.1. Experimental

In a typical separation method, shown schematically in Figure 2.8, the raw solution of gold nanorods was centrifuged at 5600 x g for 30 minutes. The bottoms and side wall residue were carefully removed via glass pipet and transferred into separate centrifuge tubes where they were each dispersed in water. A UV-Vis spectrum was collected for the supernatant, bottoms, and side wall products. The supernatant was then centrifuged for 30 minutes at 10,000 x g. The product from this second step was dispersed in water. A UV-Vis spectrum was taken for this second product and second supernatant.

2.2.2. Results and Discussion

Figure 2.9 shows the spectra of the different centrifugation products. It can be seen that the first round of centrifugation removes much of the isotropic products as indicated by the broad, blue-shifted spectrum for the bottoms product. The slightly red-shifted and narrower peak of the side wall product suggests that it contains a population of slightly longer nanorods than the supernatant.

The second round of centrifugation does not show a significant improvement over the aspect ratio of the nanorods. The TEM images in Figure 2.10 taken for the final product after the second centrifugation and the side wall product from the first centrifugation confirm that indeed a considerably lower amount of isotropic particles than from the original solution. The TEM images show that the isotropic particles typically have a larger diameter than the

nanorods. The high proportion of nanorods present in the supernatant supports the sedimentation prediction described earlier that the nanoparticles with smaller diameters do not sediment as fast as the larger nanospheres. Though not optimized, this method shows promise in concentrating the longer nanorods.

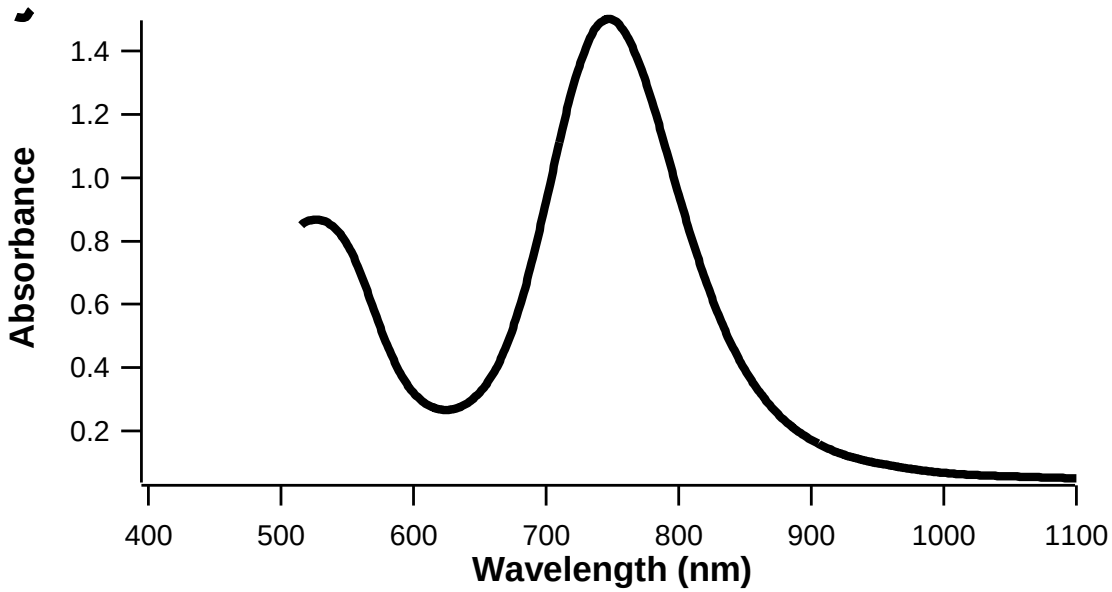

Figure 2.1. A typical UV-Vis spectrum of gold nanorods stabilized with CTAB

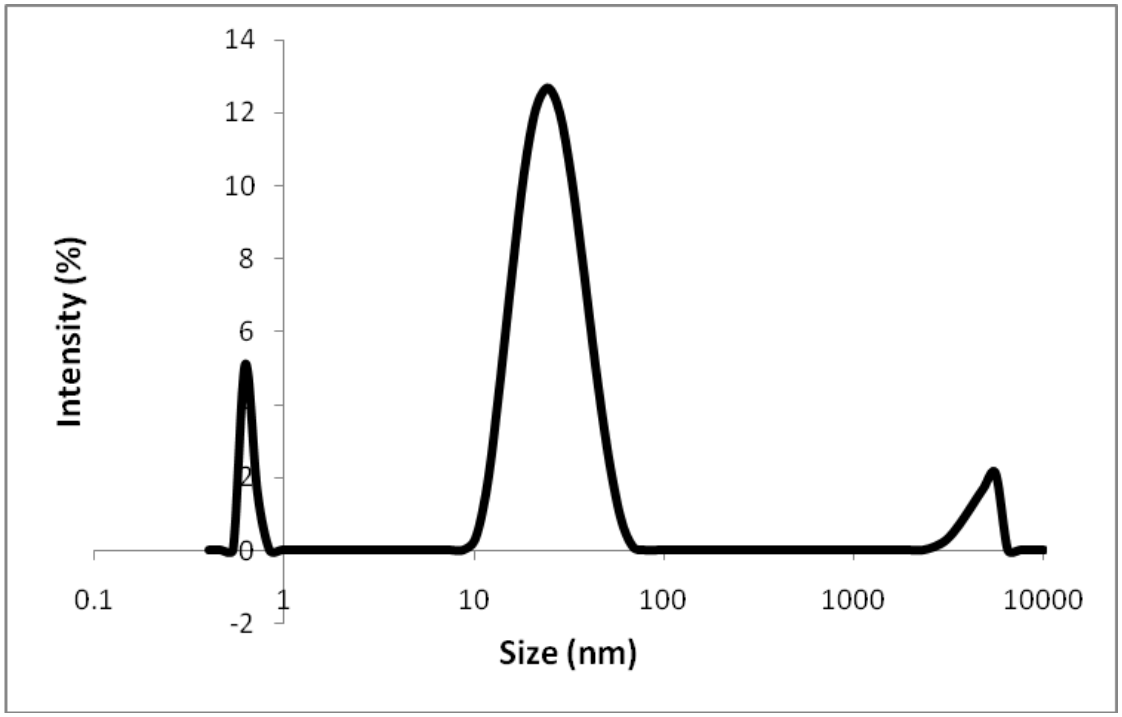

Figure 2.2. A typical DLS size distribution of gold nanorods stabilized with CTAB

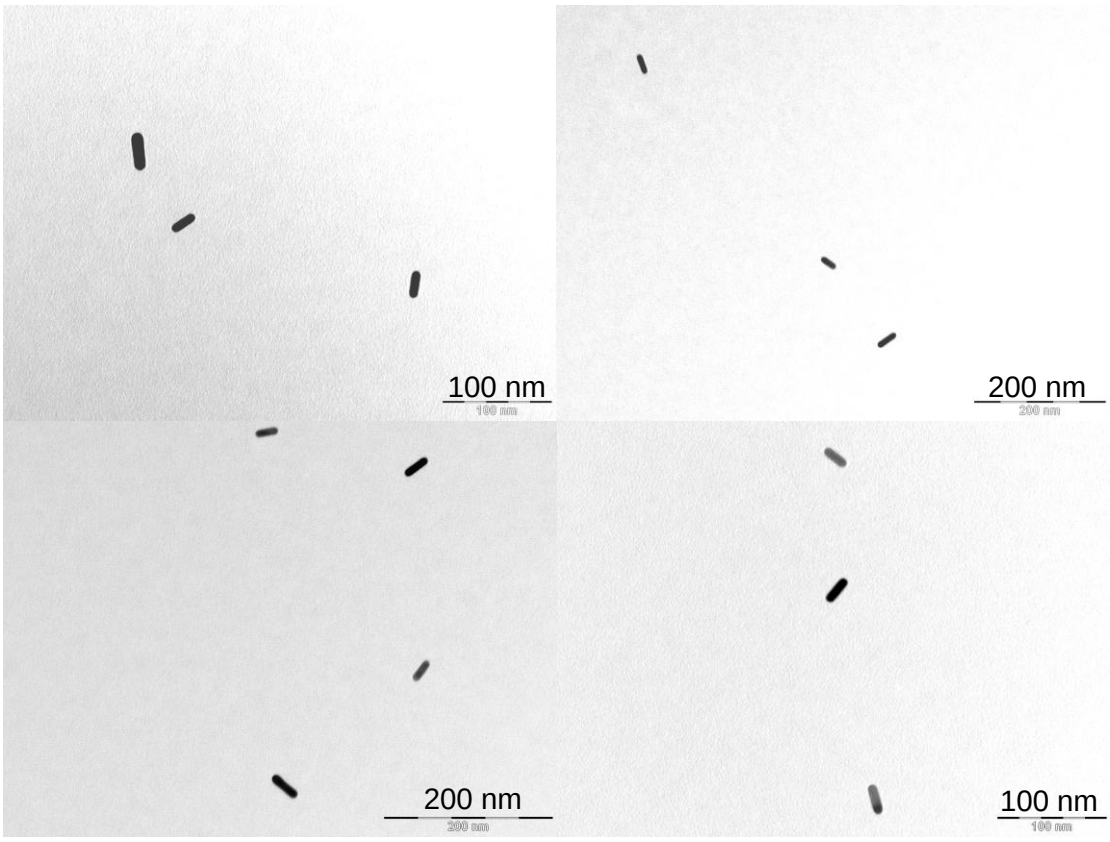

Figure 2.3. TEM images of CTAB-stabilized gold nanorods

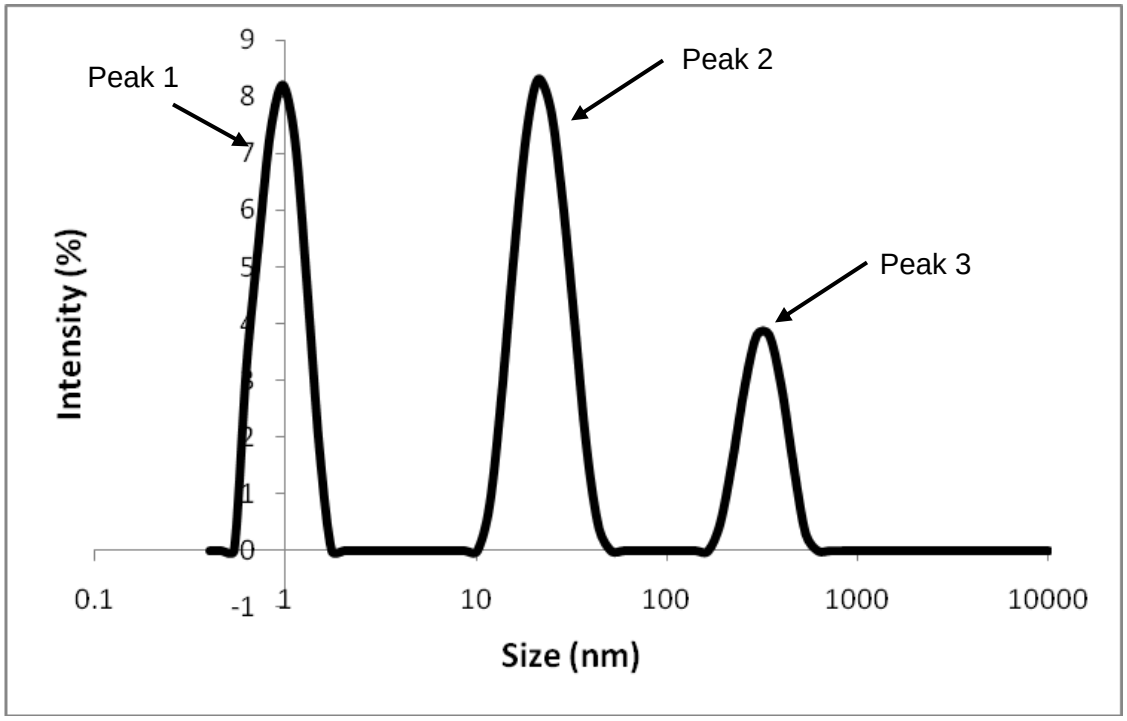

Figure 2.4. A typical DLS size distribution of gold nanorods stabilized with CTAB and BDAC. Peak 2 is referenced in Figure 2.6.

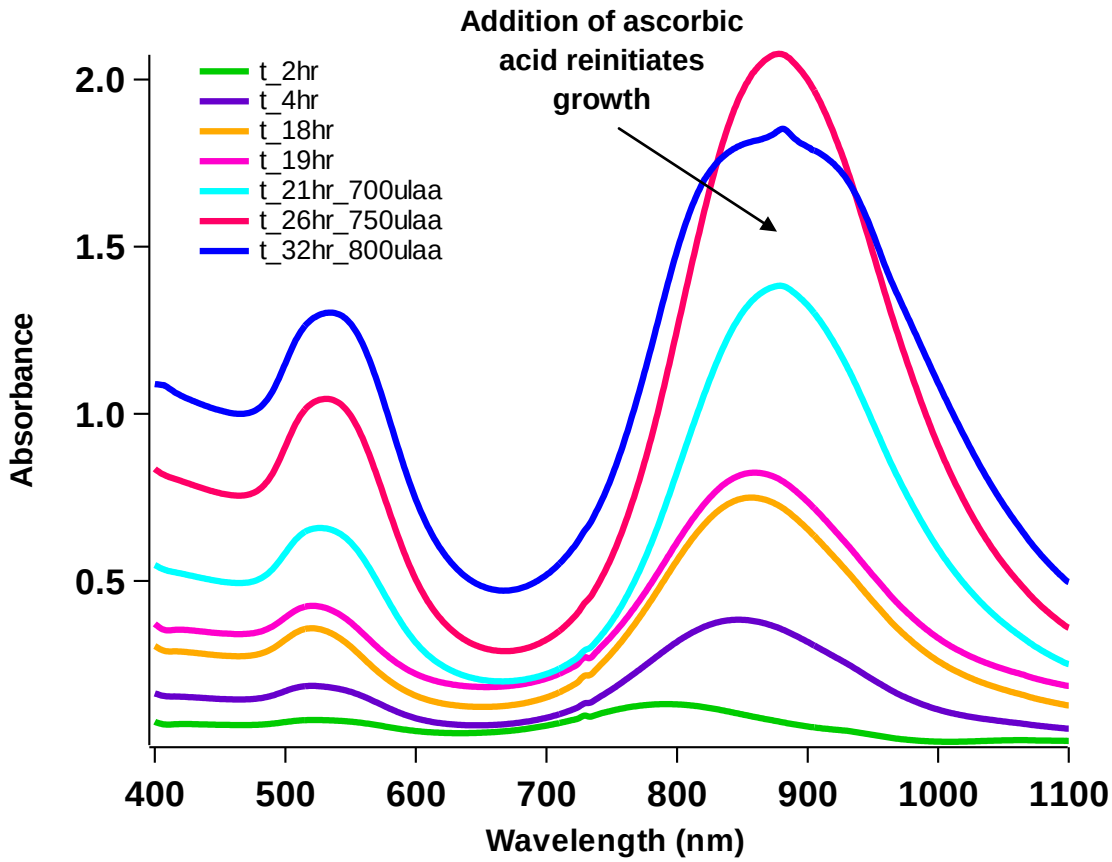

Figure 2.5. UV-Vis spectra of gold nanorods stabilized with CTAB and BDAC with the stepwise addition of ascorbic acid. The red-shifting of the peaks indicates higher aspect ratio nanorod formation.

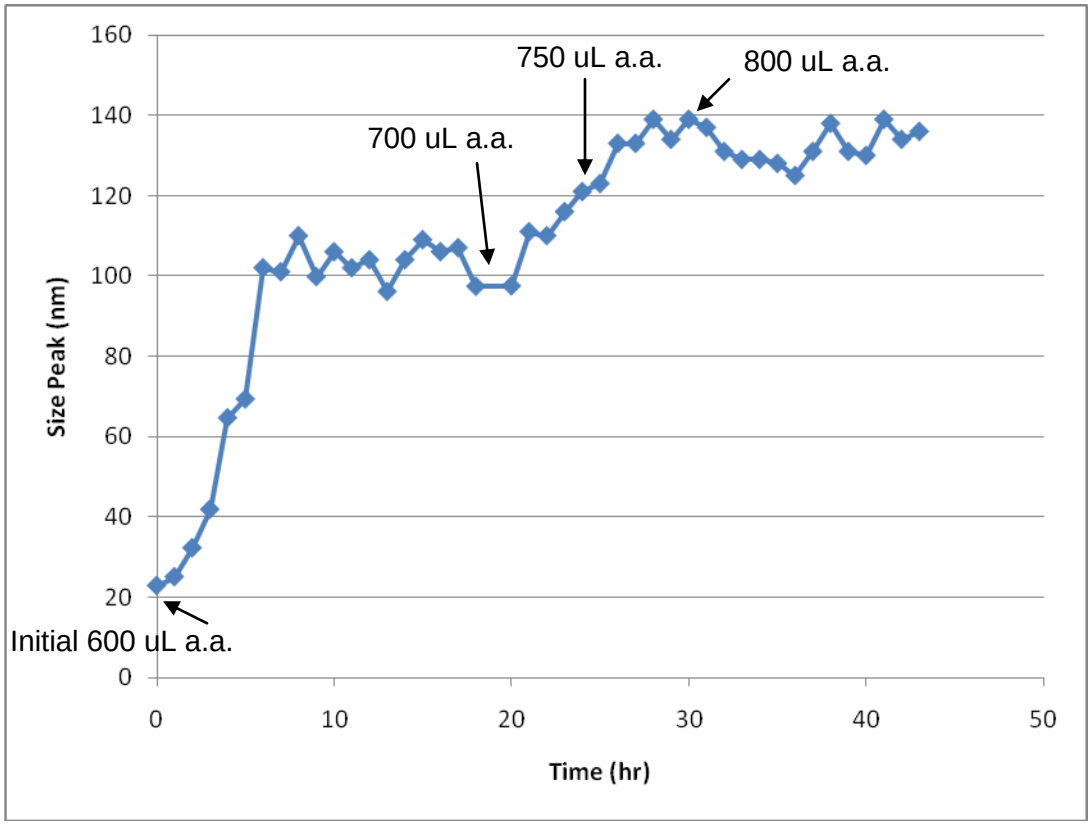

Figure 2.6. Trend graph from the DLS (Peak 2 from Figure 2.4) indicating the growth of the gold nanorods through different additions of ascorbic acid.

(a)

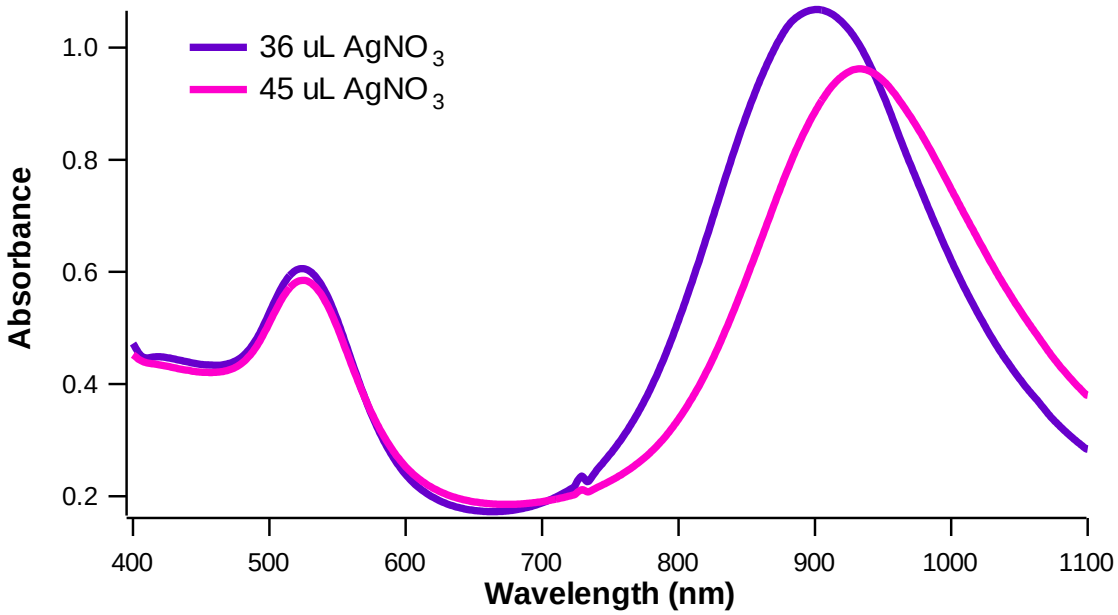

(b)

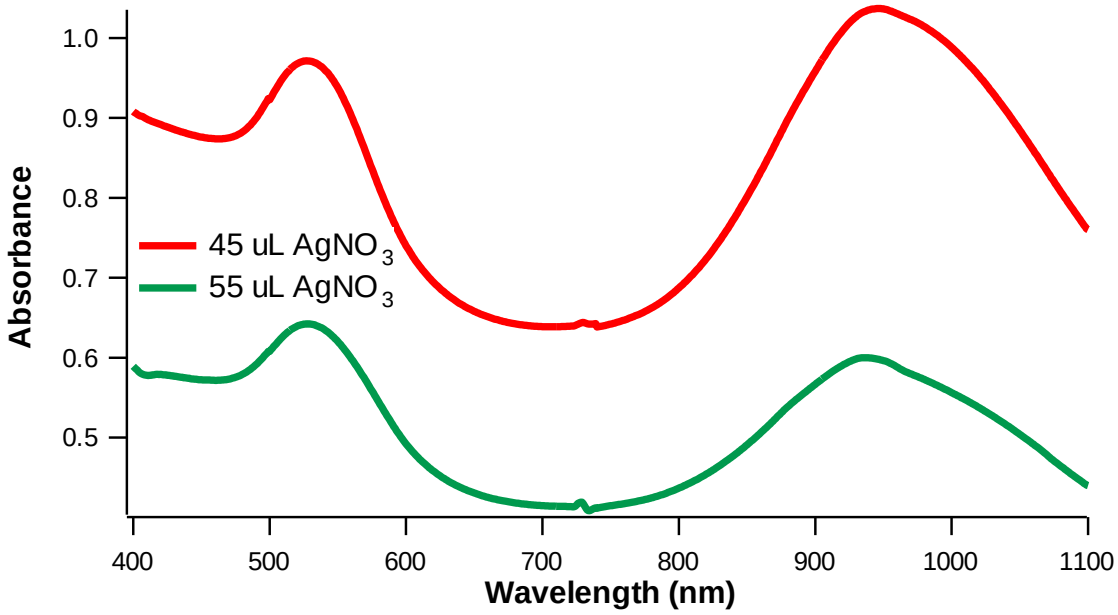

Figure 2.7. (a) UV-Vis spectra of an experiment that compares the different volumes of silver nitrate (36 µL vs. 45 µL) (b) UV-Vis spectra of an experiment that compares the different volumes of silver nitrate (45 µL vs. 55 µL).

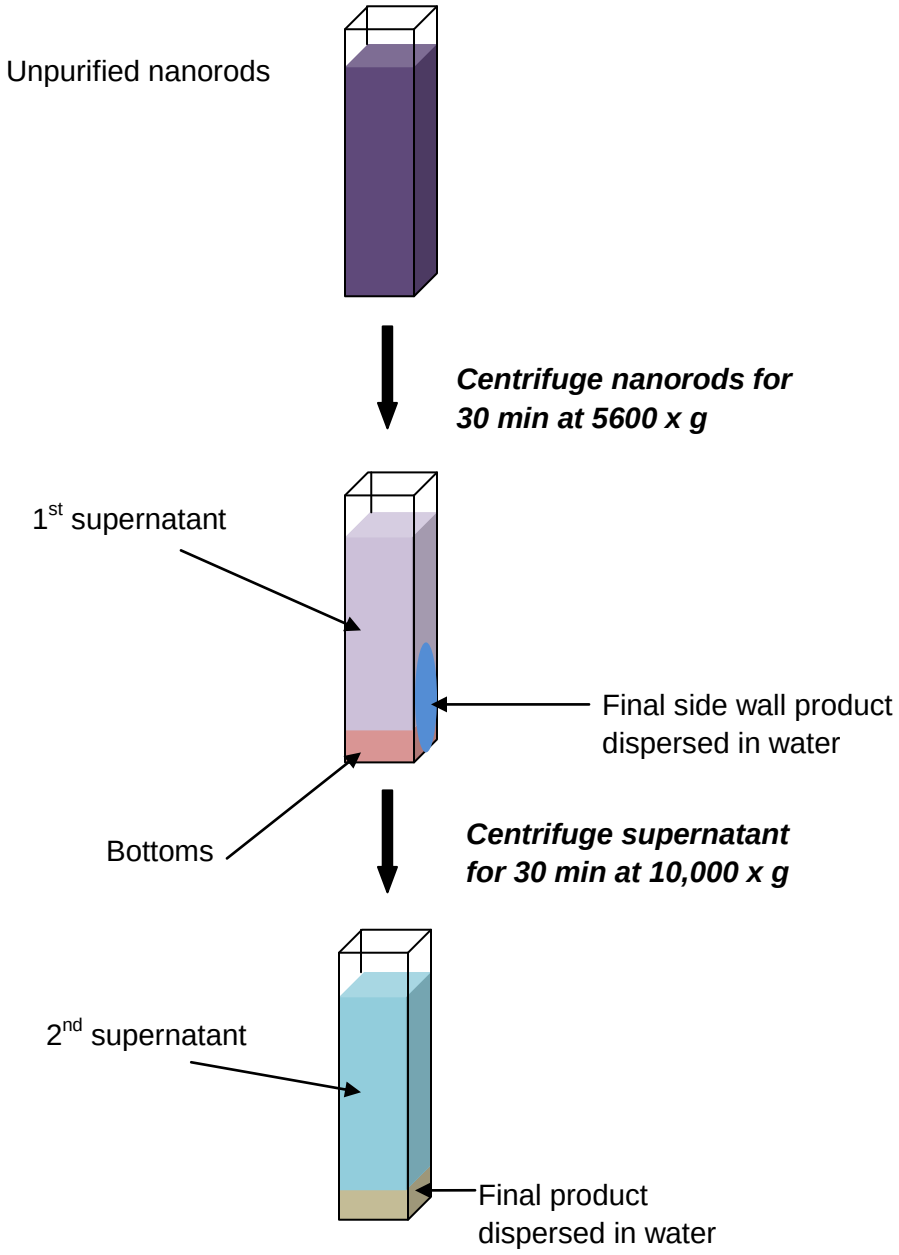

Figure 2.8. Schematic representation of a typical nanorod purification procedure.

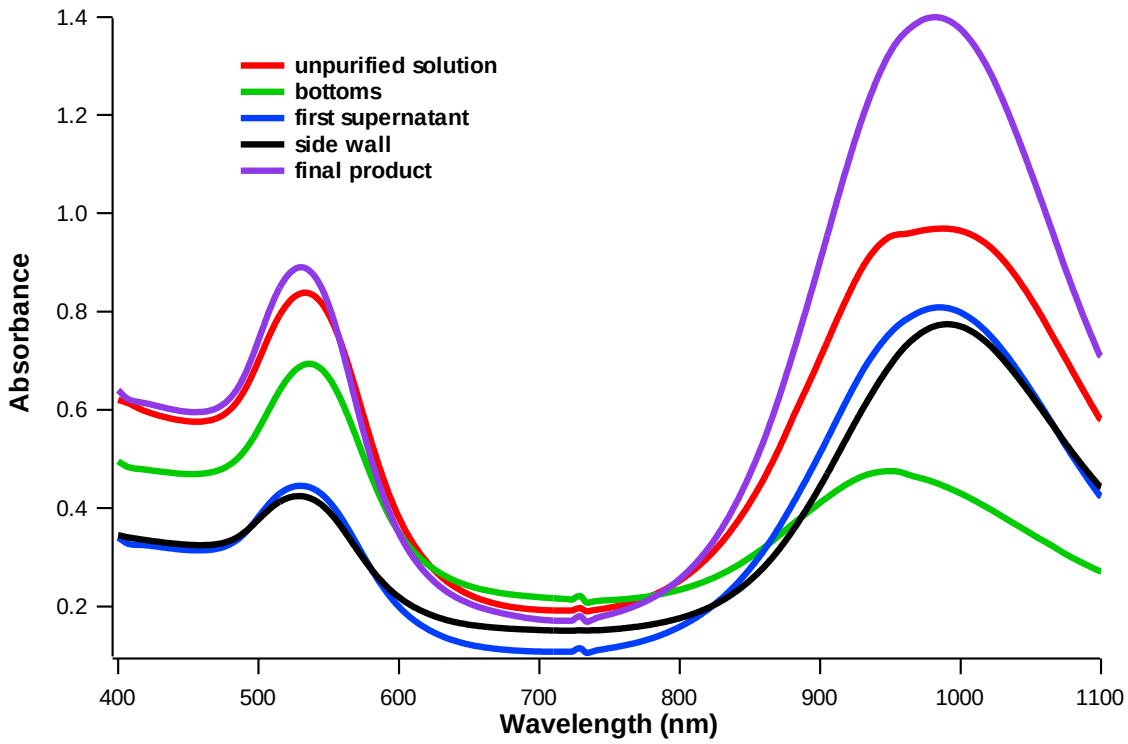

Figure 2.9. A typical UV-Vis spectra of the nanorods at various purification steps.

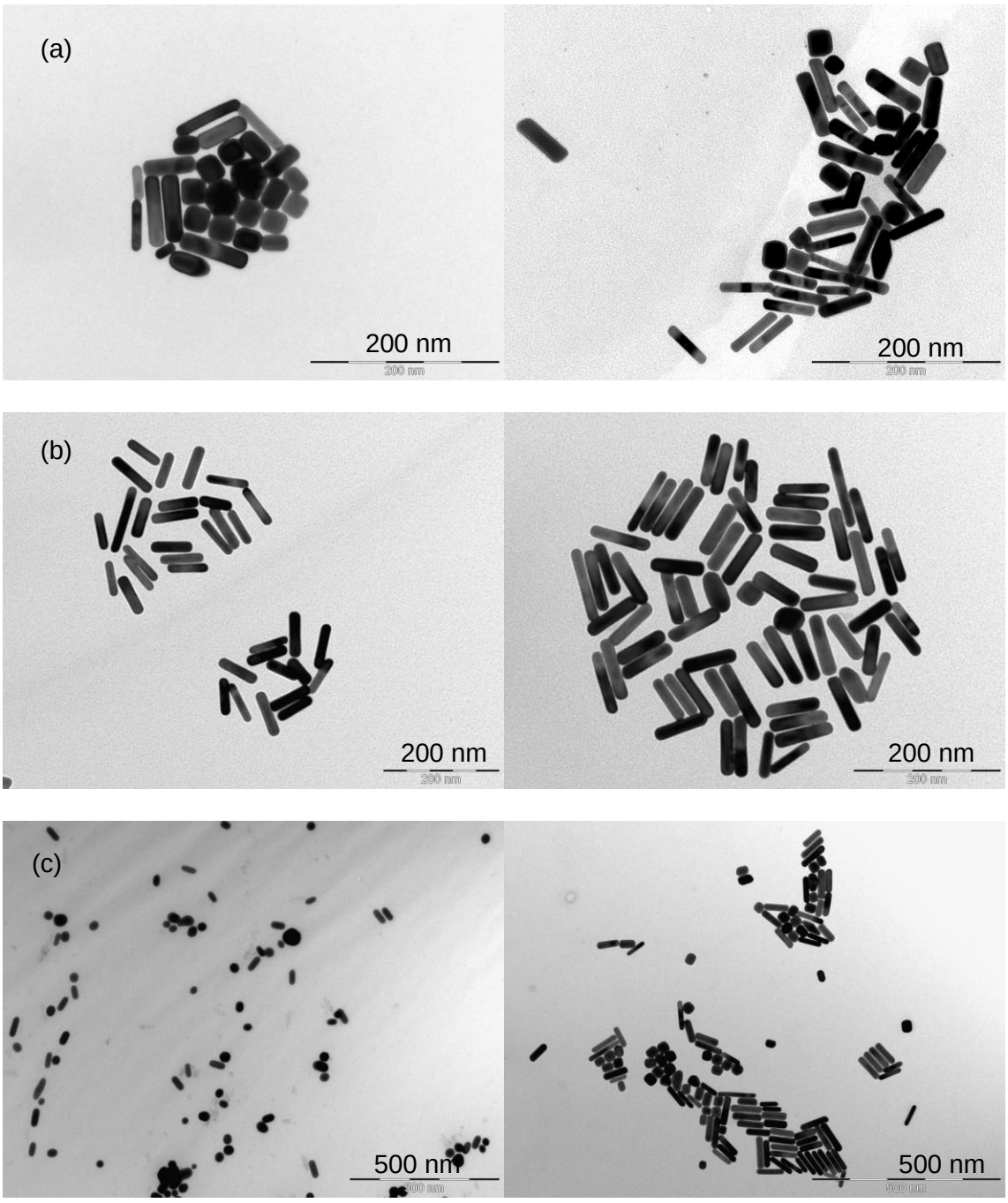

Figure 2.10. TEM images of gold nanorods at different stages of purification. (a) Nanorods purified from the supernatant. (b) Nanorods purified from the side wall residue. (c) Nanorods from the bottoms of the first centrifugation.

Chapter 3:

Self-Assembly of Gold Nanorods Using Resorcinarenes

3.1. Resorcinarene Monolayers on Gold

Understanding the properties of interfaces is essential in engineering nanostructures. For example, nanoparticles often require surface modification not only for stabilization in solution but also for attachment of different functional groups to serve a variety of applications based on particle surface interactions[33]. One way to achieve this molecular insight is through the investigation of self-assembled monolayers. A self-assembled monolayer consists of a packed arrangement of molecules whose head groups are adsorbed onto a substrate surface. Numerous systems have been studied, such as silanes on hydroxyl substrates and fatty acids on metal oxides[34].

One of the most well-known self-assembly systems is alkanethiols on gold. It has been popular in literature due to its ease of study under ambient conditions and ability to form stable monolayers owing to the high affinity of sulfur to gold. In this research, resorcinarenes with thiol groups are self-assembled on planar gold in solution. Resorcinarene monolayer formation was studied to probe the resorcinarene thiol-gold interactions that would occur during actual nanoparticle self-assembly.

The resorcinarenes used in this research were synthesized in Dr. Bisht's lab. Two types of resorcinarenes were used: one with a thiol-terminated group on

one rim (R1S) and one with a thiol-terminated group on both rims (R2S). Figures of these macrocycles are shown in Figure 3.1.

3.1.1. Experimental

3.1.1.1. Materials

Dimethylformamide (DMF) and methanol were obtained from Sigma Aldrich. Sodium hydroxide (NaOH) was purchased from Fisher Scientific. Thermally evaporated gold slides were previously prepared by Walker.

3.1.1.2. Preparation of Resorcinarene Stock Solutions

A small amount of the solid R1S was dissolved in methanol. After one minute of sonication, 2 mL of 1 M NaOH was added to the solution to deprotect the carbonyl group. DMF was added to solubilize the solid fragments. After sonication, the sample was stirred overnight in the hood at room temperature. The sample was rinsed with methanol before two rounds of centrifugation at 7500 rpm for 25 minutes. The product was dried with nitrogen and dispersed in DMF. The procedure was repeated for R2S.

3.1.1.3. Formation of Resorcinarene Monolayers on Gold

A small amount of the stock solution was transferred to a weighing bottle in DMF. A fresh gold slide was immersed in the weighing bottle solution for over 24 hours for monolayer formation.

As a control, a solution of 1 mM hexadecanethiol in ethanol was prepared for gold slide immersion.

3.1.1.4. Characterization of Resorcinarene Monolayers on Gold

Fourier transform infrared spectroscopy (FTIR) and contact angle measurements were used to characterize the resorcinarene monolayers. The gold slide was removed from the weighing bottle solution and rinsed with ethanol, followed by nitrogen drying. The photoelastic modulation setting on the FTIR was set to 3300 cm^{-1} to capture the methyl and methylene signals.

To explore the quality of monolayer formation on planar gold, a goniometer was used to measure contact angles. Solvents used were DI water and hexadecane.

3.1.2. Results and Discussion

Figure 3.2 shows the FTIR spectra of R1S monolayer formation on gold slides. The two prominent peaks are the methylene peaks at 2854 cm^{-1} and 2929 cm^{-1}. Figure 3.2 also shows the FTIR spectra of R2S monolayer formation on gold slides. The two prominent peaks are the methylene peaks at 2856 cm^{-1} and 2928 cm^{-1}. These are comparable to each other, but slighty red-shifted from the spectra belonging to the well-studied hexadecanethiol monolayer on gold, whose methylene peaks occur at 2848 cm^{-1} and 2918 cm^{-1}. This suggests a higher degree of order for the alkanethiol monolayer. Additionally, the higher absorption

for the R2S monolayer compared to the R1S and alkanethiol monolayers suggest a possible bilayer arrangement.

The contact angles with hexadecane and water for R1S, R2S, and hexadecanethiol are summarized in Table 3.1. It can be seen that the contact angles for the resorcinarene monolayers are considerably lower than for the hexadecanethiol monolayer. This is likely due to undersaturated methyl surface of the resorcinarenes, which does not provide the same degree of hydrophobicity as a hexadecanethiol monolayer does. Large values of the hysteresis (the difference between the advancing and receding angles) for water for R1S and R2S is associated with disordered surfaces[35], and this is consistent with the FTIR results.

3.2. Characterization of Self-Assembly of CTAB-Stabilized Gold Nanorods with Resorcinarenes

As described in Chapter 1, the end-to-end linkage of gold nanorods typically relies on the free {111} surface of the gold and its interaction with a ligand. CTAB-stabilized gold nanorods in water previously synthesized by Walker were used to study the self-assembly with the resorcinarenes. The nanorods were mixed with microliter amounts of the resorcinarene solutions and monitored over time with DLS, UV-Vis spectroscopy, and TEM.

3.2.1. Experimental

3.2.1.1. Materials

The gold nanorods coated with CTAB were previously synthesized by Walker, and the resorcinarenes were synthesized in Dr. Bisht's lab. Water used for all experiments is from EasyPure UV System (from Barnstead, IA), where particulate matter was removed via a 0.2 μm filter.

3.2.1.2. Time Studies of Self-Assembly of CTAB-Stabilized Gold Nanorods

UV-Vis spectroscopy, DLS, and TEM were used to monitor the self-assembly of the gold nanorods over time for up to six hours. In a polystyrene cuvette, 150 μL of the gold nanorods were mixed with 850 μL of DI water. After the t=0 measurements, different amounts of the R2S/DMF stock solution (5 μL, 10 μL, and 20 μL) were added to the cuvette in separate experiments. A control experiment was performed with the gold nanorods and DMF to verify that linking would be due to the resorcinarenes and not due to the solvent.

Additionally, the effects of initial vs. constant mixing was explored. Initial mixing occurred after the introduction of the resorcinarene and took place by a few inversions of the cuvette solution. A vortexer set at a low speed was used to simulate constant mixing during experimentation.

Experiments were repeated for the R1S-gold nanorod system.

3.2.2. Results and Discussion

Figure 3.3 shows a typical UV-Vis spectrum of gold nanorod self-assembly via both R1S and R2S. Within one hour, it can be seen that there is a larger red-shift and a broader peak shape for the R2S than for the R1S. This is to be expected since linking with the R2S would occur in a more straightforward manner with the sulfur groups on both ends serving to bridge together adjacent nanorods. As mentioned earlier, a red-shift in the absorption spectra for gold nanoparticles is attributed to interparticle plasmon coupling. Thus, the higher peak absorption for the self-assembly by R2S at around 780 nm suggests longer chains. The red-shift for the R1S-mediated assembly indicates that the R1S with only one thiol-terminated rim was able to link up the nanorods. The control experiment with only the addition of DMF verifies that self-assembly is due to the resorcinarenes.

TEM images shown in Figure 3.4 confirm the self-assembly of the nanorods. From the images, it becomes difficult to visually distinguish the difference in the two assemblies. Information provided by the DLS may be a better way to differentiate between the two resorcinarenes. In Figure 3.5, the autocorrelation plot is presented for both systems in comparison to the initial time. An interesting trend is observed for the autocorrelation function graph: the curve for the nanorod assembly due to R1S is bi-exponential, while the curve for the nanorod assembly due to R2S is a single exponential. This behavior was observed regardless of the different concentrations of the resorcinarenes.

3.3. Characterization of Self-Assembly of CTAB/BDAC-Stabilized Gold Nanorods with Resorcinarenes

In addition to the CTAB-stabilized nanorods, longer gold nanorods synthesized with a two-surfactant system of CTAB and BDAC were used to look at the self-assembly with the resorcinarenes. The nanorods were mixed with microliter amounts of the resorcinarene solution and monitored over time with DLS, UV-Vis spectroscopy, and TEM. Water used for all experiments is from EasyPure UV System (from Barnstead, IA), where particulate matter was removed via a 0.2 μm filter.

3.3.1 Experimental

3.3.1.1. Materials

The gold nanorods synthesized using the binary surfactant system described in Chapter 2 were used. Water used for all experiments was obtained from EasyPure UV System (from Barnstead, IA), where particulate matter was removed via a 0.2 μm filter.

3.3.1.2. Time Studies of Self-Assembly of CTAB/BDAC-Stabilized Gold Nanorods

In a polystyrene cuvette, 300 μL of the gold nanorods were mixed with 695 μL of DI water. After the t=0 measurements, a diluted amount of the R2S stock solution (corresponding to about 0.25 μL of the original stock) was added to the

cuvette. UV-Vis spectroscopy, DLS, and TEM were used to monitor the self-assembly of the gold nanorods over time for up to four hours.

3.3.2. Results and Discussion

Figure 3.6 shows a UV-Vis spectra of the CTAB/BDAC gold nanorod self-assembly via R2S. Unlike what was observed in the CTAB-only nanorod system, the absorption spectra show no red shifts. A slight blue shift was witnessed instead. TEM images in Figure 3.7 show no linear self-assembly. Rather, they show aggregation of the nanorods. It could be that the aggregation had happened in solution during the experiment, but due to the largely non-linear assembly, the spectra had blue-shifted instead. The experiment was repeated with a different batch of the nanorods and showed similar results.

A separate experiment was done using the same resorcinarene stock solution on CTAB-stabilized gold nanorods to ensure the quality of the R2S was not a problem. The results were similar to earlier typical self-assembly experiments of R2S with CTAB-stabilized gold nanorods. Though further experimentation would need to be done, these findings suggest that there may be something else in the binary surfactant system that prevents end-to-end assembly.

However, a review of current literature on gold nanorods synthesized with BDAC and CTAB does not reveal any difference in nanorod crystallography arising from the binary surfactant synthesis compared to the more common CTAB-mediated methods[15-31]. Few researchers use the binary surfactant system

as their synthesis of choice so there is still work that remains to be explored in order to better understand how the surfactants, reagents, and the gold surfaces interact with each other.

(a) (b)

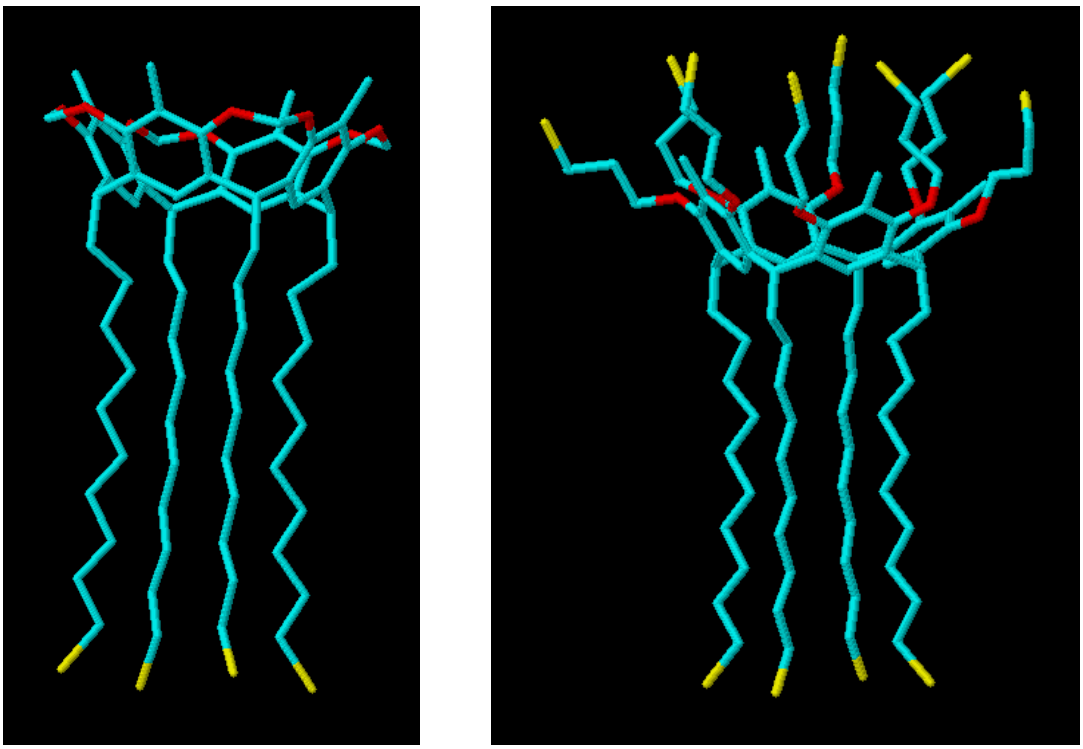

Figure 3.1. (a) Schematic of R1S and (b) schematic of R2S

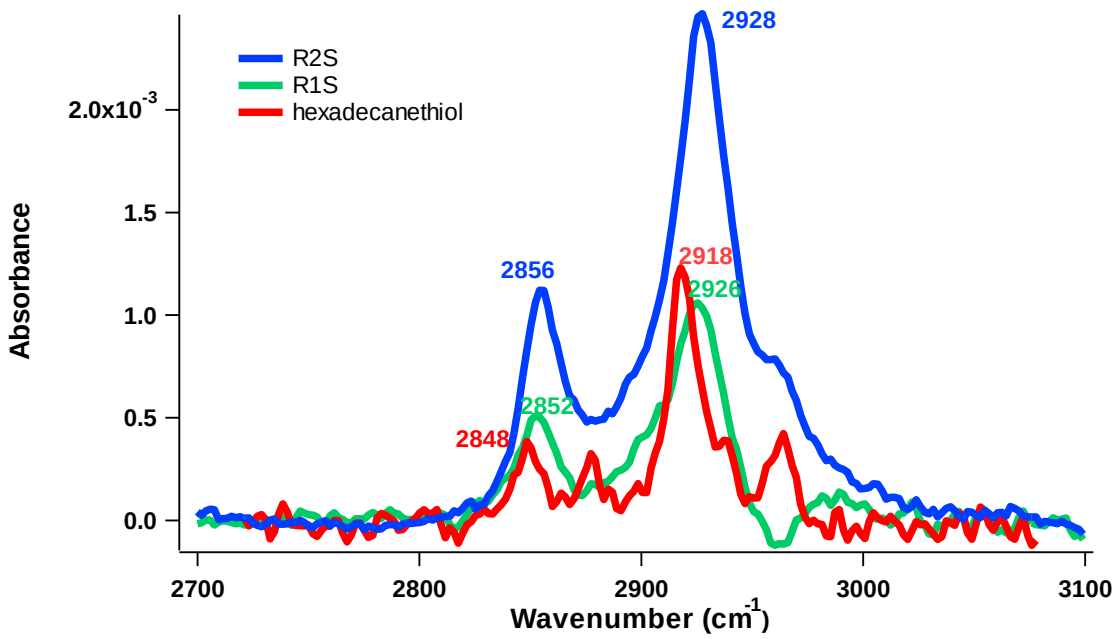

Figure 3.2. FTIR spectra of self-assembled R1S and R2S monolayers on gold compared to hexadecanethiol on gold.

Table 3.1. Contact angles for self-assembled monolayers on gold for R1S, R2S, and hexadecanethiol.

Monolayer	Average Advancing Angle for Water	Average Receding Angle for Water
R1S	74°	56°
R2S	89°	77°
**C_{16}SH	112°	105°

Monolayer	Average Advancing Angle for Hexadecane	Average Receding Angle for Hexadecane
R1S	<10°	<10°
R2S	<10°	<10°
C_{16}SH	44°	38°

** source: Bain et al., *J. Am. Chem. Soc.*, 1989, 111 (1), 321-335 and Labinis et al., *J. Am. Chem. Soc.*, 1991, 113 (19), 7152-7167 .

(a)

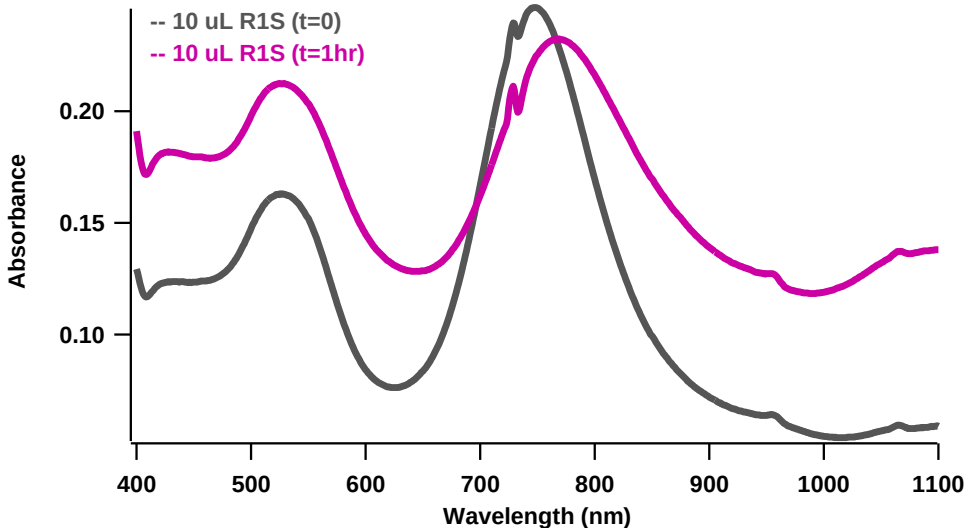

(b)

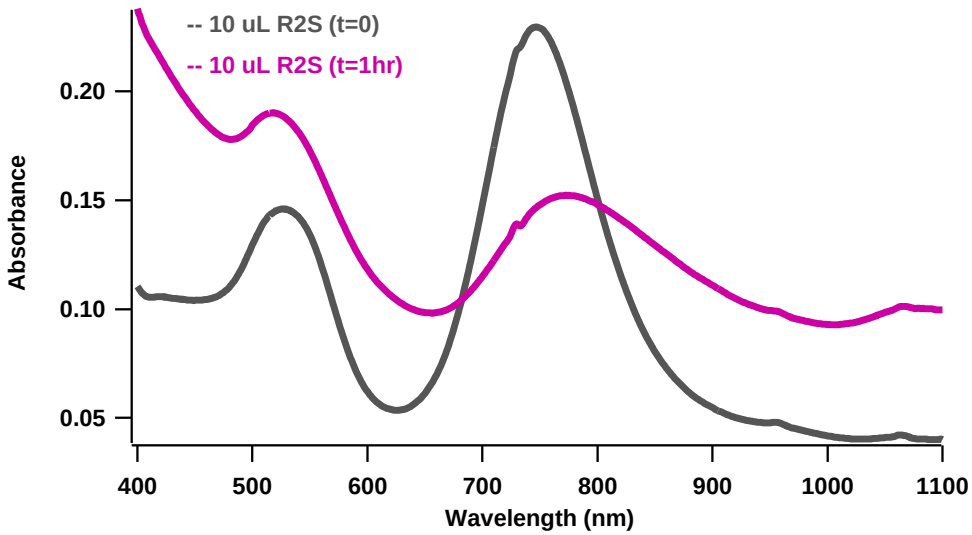

Figure 3.3. UV-Vis spectra of R1S and R2S in the self-assembly of CTAB-stabilized gold nanorods.

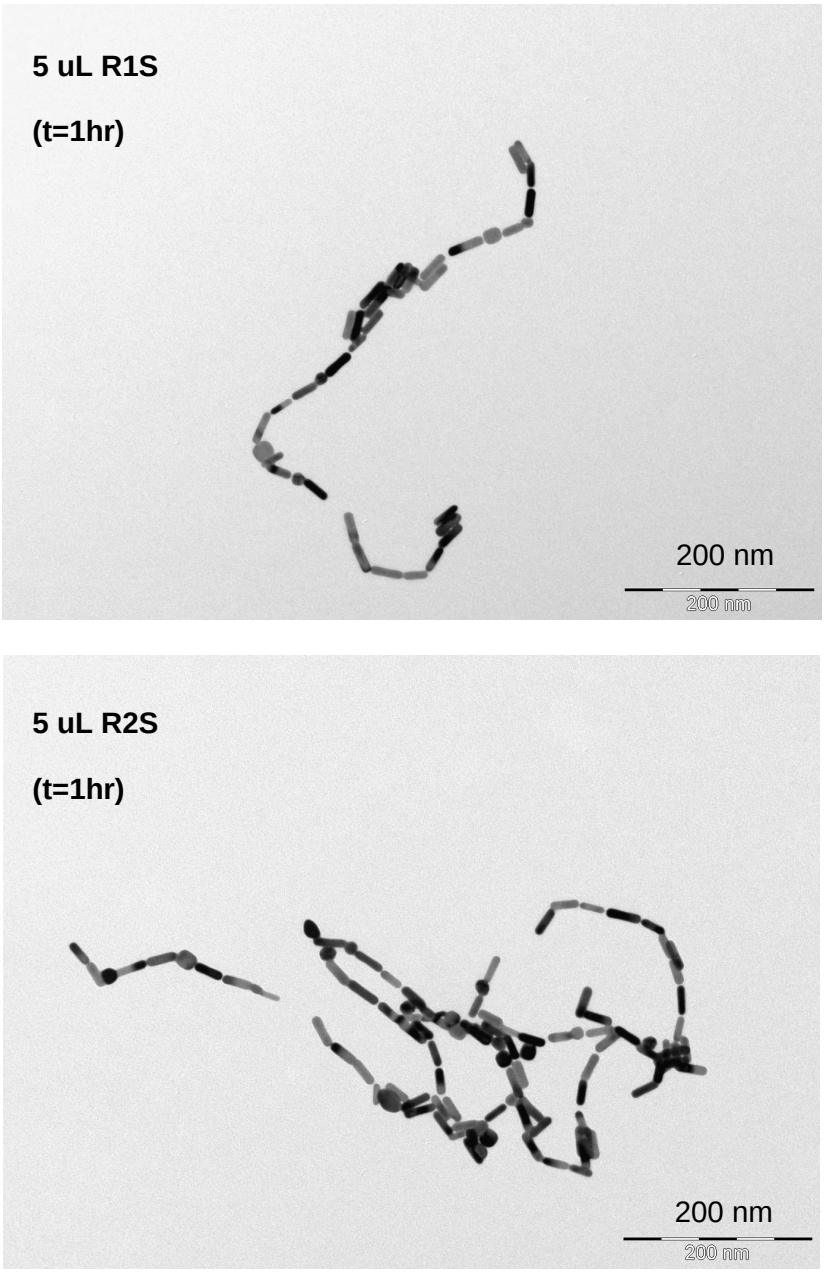

Figure 3.4. TEM images of the self-assembly of CTAB-stabilized nanorods by resorcinarenes.

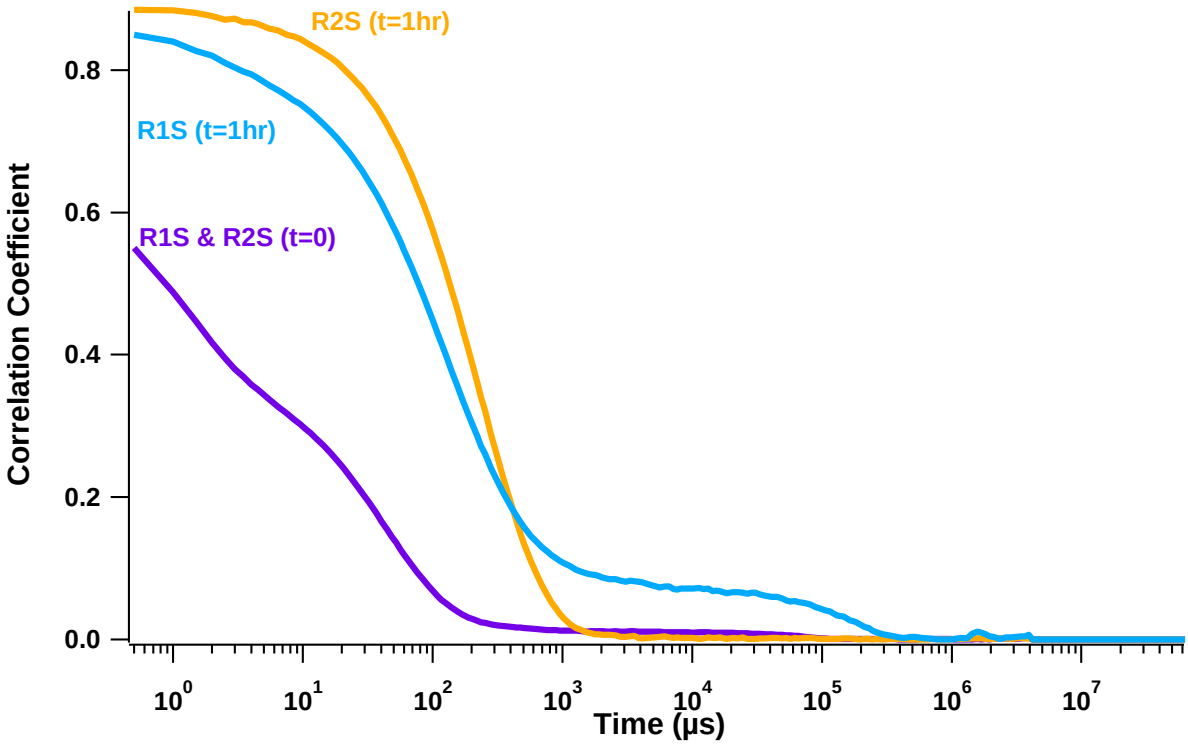

Figure 3.5. DLS autocorrelation plot of CTAB-stabilized nanorod linkage by R1S and R2S over time. Chaining due to R1S manifests itself in a bi-exponential decay, whereas self-assembly mediated by R2S shows a single exponential decay.

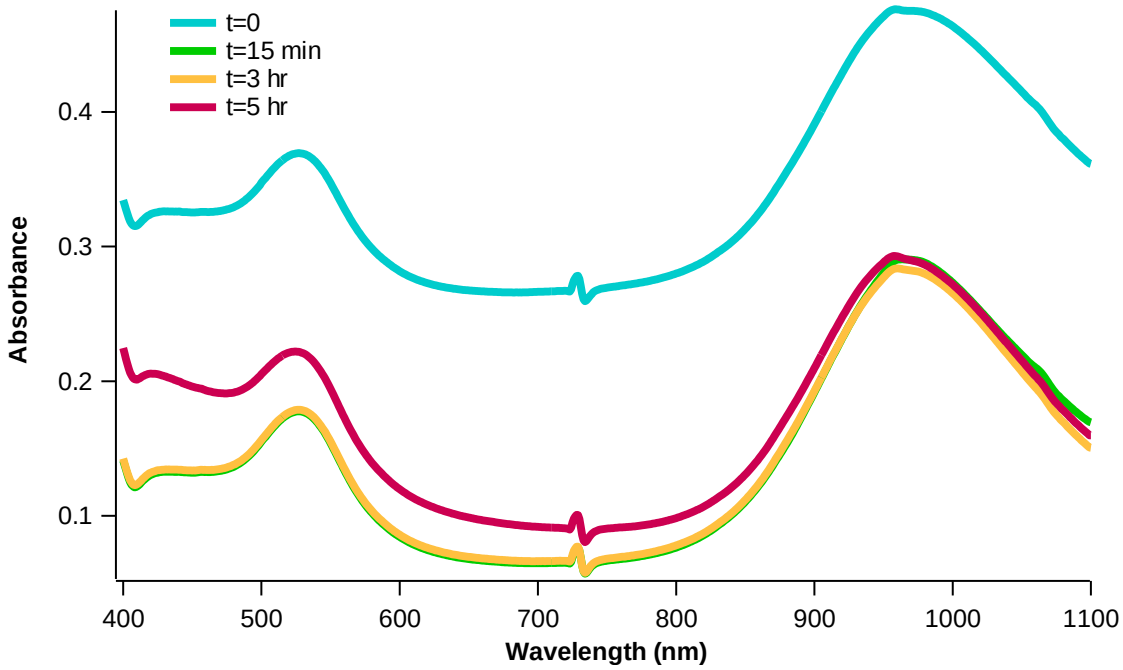

Figure 3.6. UV-Vis spectra of self-assembly of nanorods stabilized with BDAC and CTAB

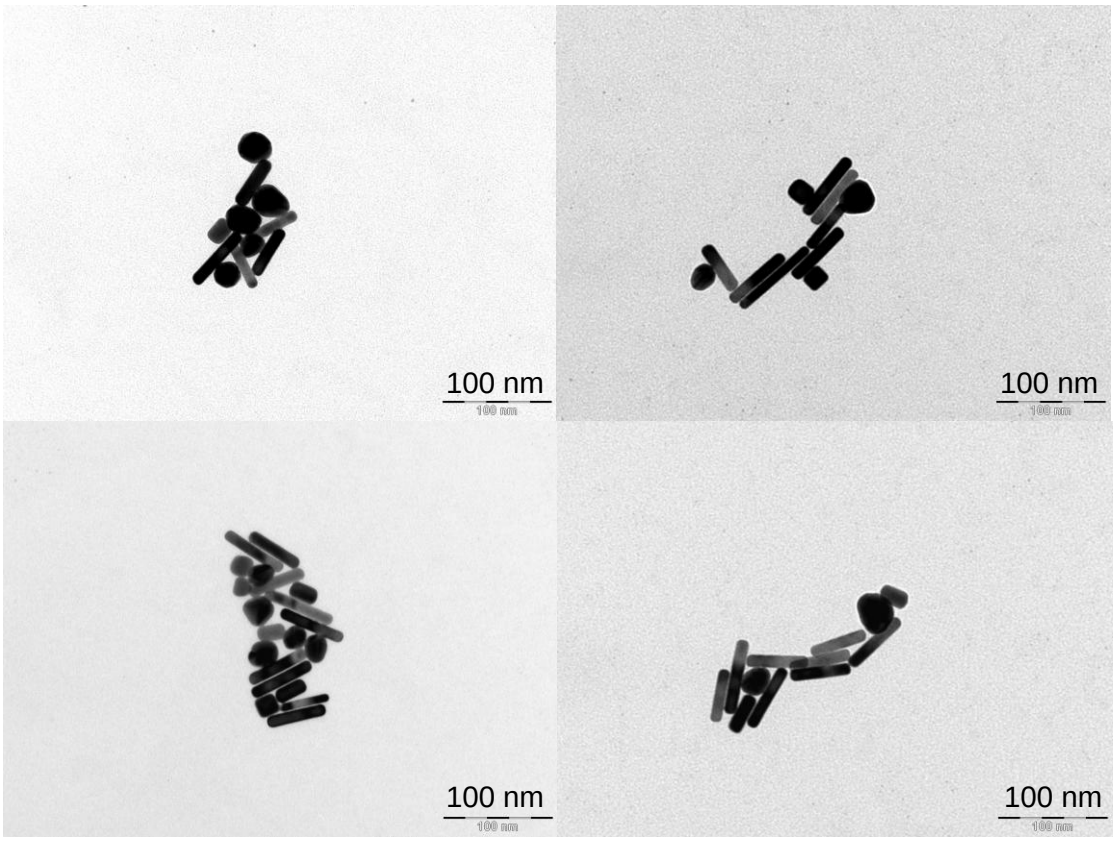

Figure 3.7. TEM images of the self-assembly of CTAB/BDAC nanorods with R2S

Chapter 4:

Synthesis and Self-Assembly of Gold Nanoprisms

4.1. Synthesis of Gold Nanoprisms

As mentioned in Chapter 1, the physical parameters of nanomaterials can influence its properties. A few changes in experimental conditions can lead to the formation of different anisotropic shapes and sizes. Among these, triangular gold nanoprisms are becoming of great interest. Various protocols for synthesizing these unique structures can be easily found in literature. The surfactant-mediated direction employed to synthesize nanorods in Chapter 2 was extended to produce gold nanoprisms. By introducing trisodium citrate and an approach towards kinetic control, CTAB-stabilized gold nanoprisms were synthesized in an aqueous solution.

The synthesis protocol used in this research was adapted from Chu and co-workers[21, 36]. The preparation route involved a thermal reduction of $HAuCl_4$ as the gold precursor in trisodium citrate and CTAB in a heating mantle. After purification, the nanoprisms were characterized with UV-Vis spectroscopy and TEM.

The mechanism for nanoprism growth using this kinetically-controlled method is proposed by Huang and colleagues[36]. They postulate that large, branched aggregates are produced within the first few seconds of reaction. The core of these aggregates increases in size as gold is reduced. Meanwhile, the

branches are growing and consolidating to form a well-defined, triangular nanoprism[36].

4.1.1. Experimental

4.1.1.1. Materials

CTAB was obtained from TCI America. Trisodium citrate was obtained from Acros Organics. The heating mantle was purchased from Cynmar. A variac transformer (from Action Electronics) was used to control the voltage input to the heating mantle.

4.1.1.2. Kinetically-Controlled Reduction Synthesis of Nanoprisms

A 7.5 mL solution of 1.67×10^{-3} M aqueous trisodium citrate and a mixture of 1.25×10^{-3} M $HAuCl_4$ and 7.5×10^{-3} M CTAB was heated to 68°C and then mixed before heating in a sand bath at 95°C. The pale orange color of the mixed solution turned colorless after two minutes. After five minutes, the solution turned a light blue, indicating formation of the nanoprisms. The reaction vial was separated from the heat and allowed to cool down to room temperature. Brown residue was observed to have precipitated at the bottom of the vial. The light blue solution was carefully removed via glass pipet and transferred to a centrifuge tube, and a UV-Vis spectrum was taken of the as-made solution.

4.1.1.3. Purification of Nanoprisms

The nanoprism solution was centrifuged for ten minutes at 1500 rpm to remove the largest particles which precipitated as a dark blue layer. A UV-Vis spectrum was taken of the resulting light blue supernatant before it was transferred to another centrifuge tube and dispersed in 5 mL of 1 mM CTAB. A second round of centrifugation at 3000 rpm for 15 minutes was done, and the product was dispersed in DI water for an absorption reading. TEM images were taken of the product after each stage of purification.

4.1.2. Results and Discussion

The spectra of the nanoprisms in Figure 4.1 show a peak at 625 nm, whose location and shape are similar to that published by Huang and co-workers[36]. The peak in this region is said to be related to the thickness of the nanoprisms[36]. TEM images in Figure 4.2 show well-defined triangular nanoprisms that are range from around 80-200 nm. Though nanoprisms make up a large part of the population, anisotropic byproducts include hexagonal and long nanorods.

4.2. Self-Assembly of Gold Nanoprisms with R1S and R2S

To date, there have not been reports of gold nanoprism linking by thiol-bearing ligands. Similar to the self-assembly studies with gold nanorods and the resorcinarenes detailed in Chapter 3, the nanoprisms were mixed with microliter

amounts of the resorcinarene solution and monitored over time with DLS, UV-Vis spectroscopy, and TEM.

4.2.1. Experimental

In a polystyrene cuvette, 1 mL of an aqueous nanoprism mixture. After the t=0 measurements, a diluted amount of the resorcinarene stock solution (corresponding to about 0.25 µL of the original stock) was added to the cuvette. UV-Vis spectroscopy, DLS, and TEM were used to monitor the self-assembly of the gold nanorods over time for up to four hours.

4.1.2. Results and Discussion

The spectra of the self-assembled nanoprisms with the resorcinarenes is shown in Figure 4.3. Over a period of two hours, the optical shift in the spectra suggest that R2S linking is taking place. However, R1S-mediated assembly does not appear to occur based on the UV-Vis spectra. In both cases, TEM images (Figure 4.4) show aggregations that warrant further study.

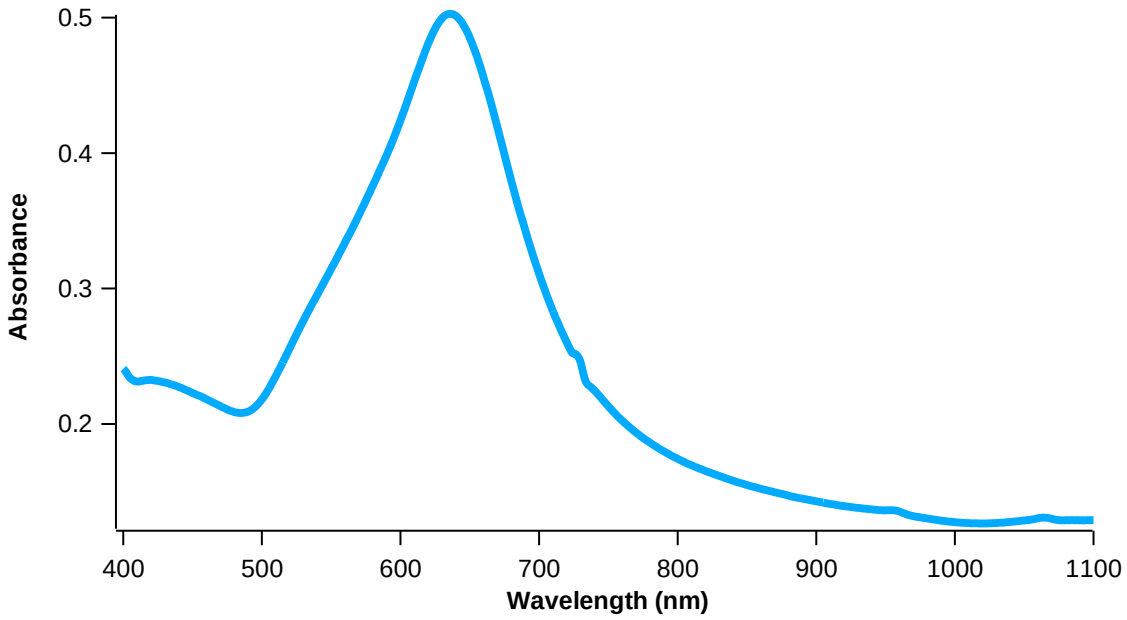

Figure 4.1. A typical UV-Vis spectrum of gold nanoprisms in an aqueous solution synthesized using a thermal reduction method

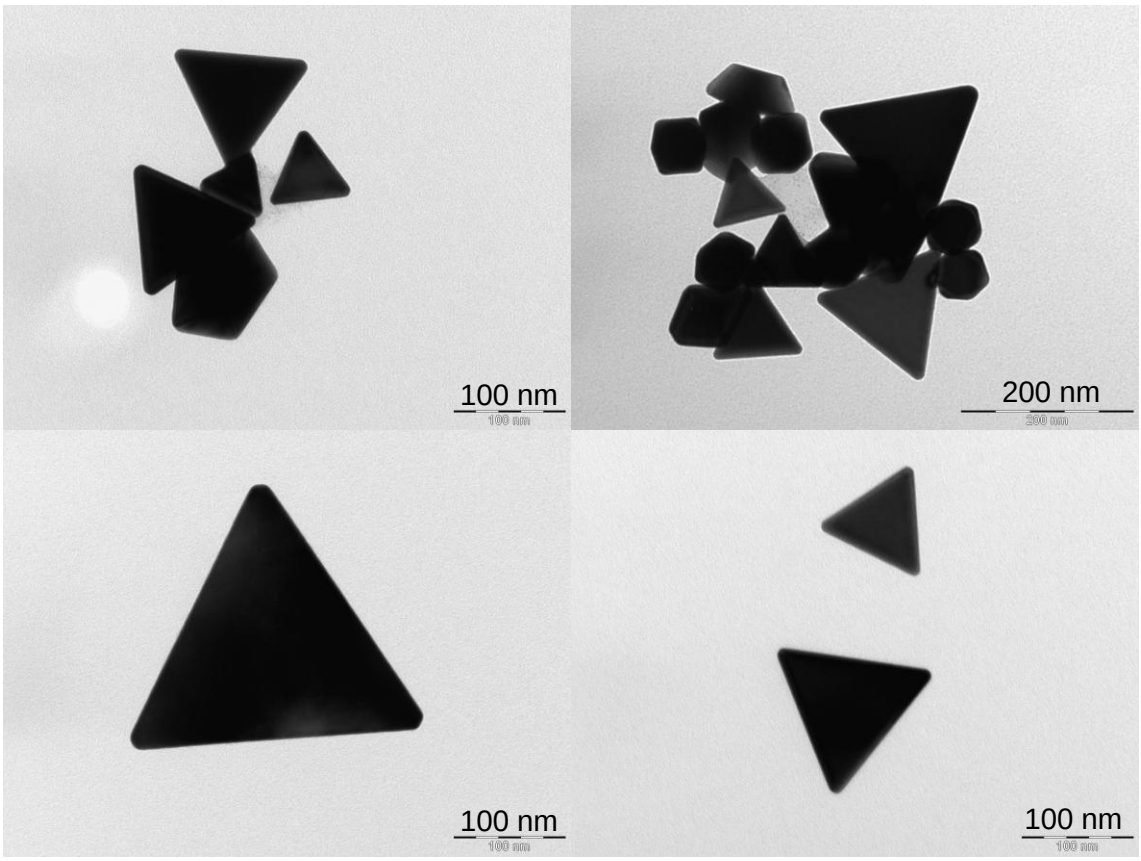

Figure 4.2. TEM images of gold nanoprisms in an aqueous solution synthesized using a thermal reduction method

(a)

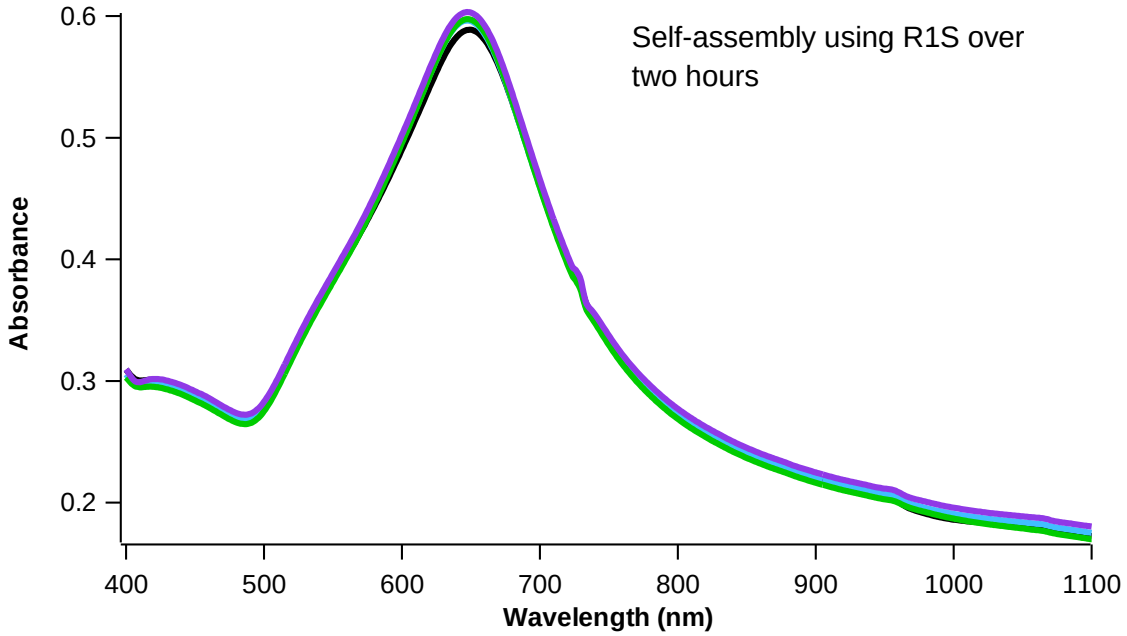

(b)

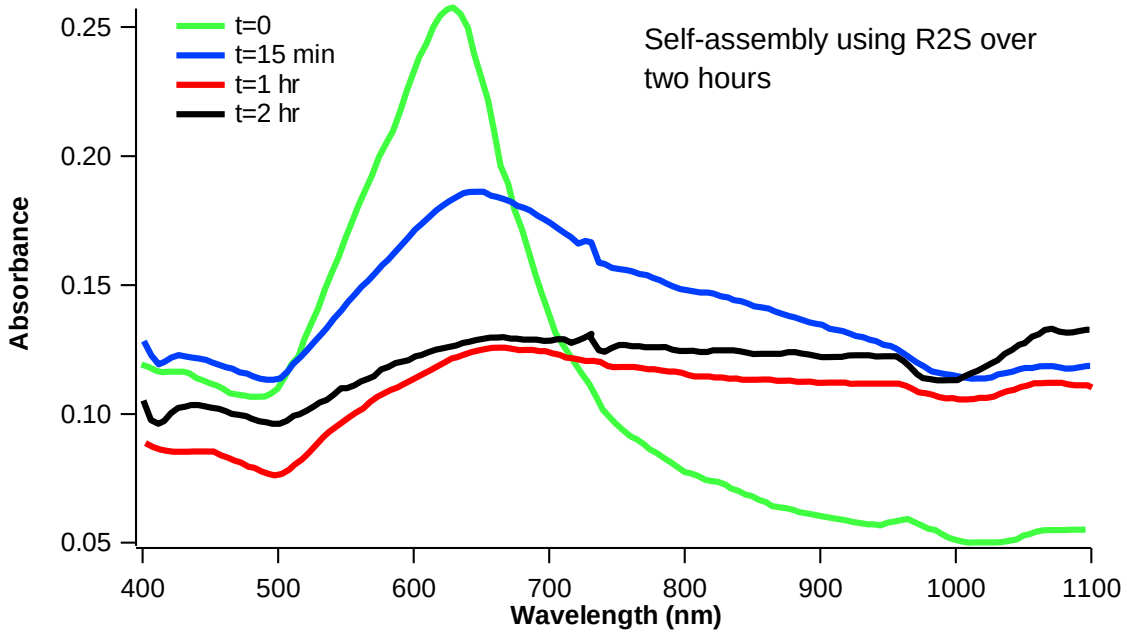

Figure 4.3. UV-Vis spectra of (a) self-assembly of nanoprisms using R1S and (b) self-assembly of nanoprisms using R2S

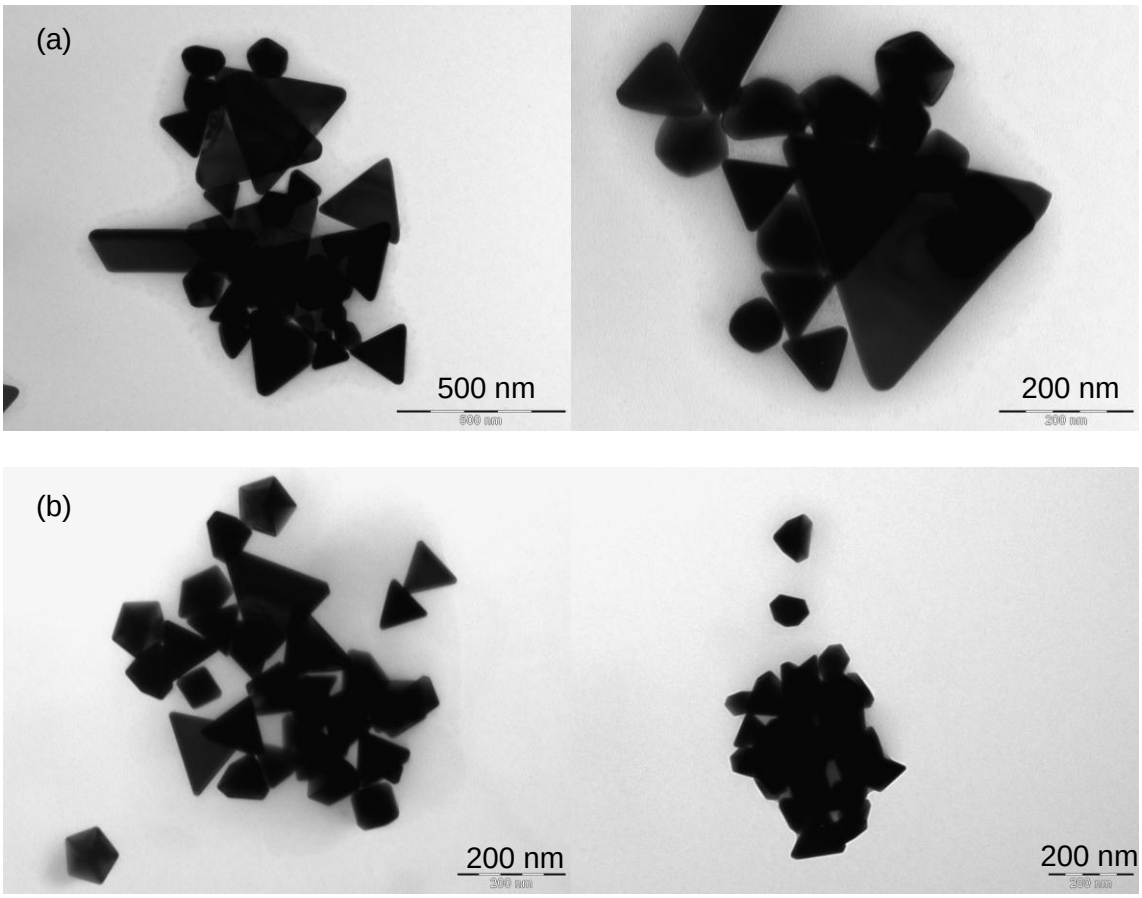

Figure 4.4. TEM images of (a) self-assembly of nanoprisms using R1S and (b) self-assembly of nanoprisms using R2S.

Chapter 5:

Summary of Research

The synthesis of gold nanorods with CTAB and BDAC has shown to be effective in producing nanorods with higher aspect ratios than those stabilized with CTAB alone. The CTAB/BDAC nanorods have an aspect ratio of 4, whereas the CTAB-stabilized nanorods originally synthesized by Walker have an aspect ratio of 3. The control over increasing the aspect ratio of the nanorods was demonstrated with the slow addition of ascorbic acid over time as well as increasing the quantity of silver nitrate.

To achieve low polydispersity of the CTAB/BDAC gold nanorods, concentration was given to the centrifugation process. It was found that two rounds of purification were required to remove much of the spherical nanoparticles from the original solution. The absorption spectra and TEM images both verify that the longer nanorods reside in the supernatant and the side wall reside after the first purification.

The self-assembled resorcinarene monolayers on gold appear to be more disordered and more hydrophilic than hexadecanethol monolayers on gold as revealed by FTIR spectroscopy and contact angle measurements.

Self-assembly of CTAB-stabilized gold nanorods with resorcinarenes produces noticeable longitudinal red-shifts in the optical spectra due to uniaxial plasmon coupling within one hour. In addition, TEM shows linking of the

nanorods with both resorcinarenes. However, these methods were unable to distinguish between R1S and R2S. It is in the autocorrelation functions that a marked difference between the two is seen based on the behavior of the decay curves. R1S exhibited a bi-exponential decay, while R2S showed a single exponential decay.

End-to-end self-assembly of CTAB/BDAC-stabilized nanorods using resorcinarenes was not seen in the UV-Vis spectra. TEM images showed nanorod aggregates. This suggests that the two-surfactant system may have a deterrent role in the linking of the nanorods.

Gold nanoprisms are a relatively new area in the field of anisotropic metallic nanoparticles. The need to understand their properties and uses in potential applications is growing. In this thesis, surfactant-mediated shape control was successful in producing gold nanoprisms. The synthesis method involved controlling the reduction kinetics of the gold precursor at high temperatures (around 95°C). The resulting structures show a peak around 625 nm and are well-defined as shown by TEM images. The self-assembly of nanoprisms by the resorcinarenes yield results that need to be further studied. Linking using R1S as shown in the non-changing UV-Vis spectra does not appear to happen, whereas linking using R2S undergoes an optical shift over time, indicating self-assembly. At this point, the TEM images reveal aggregation of the nanoparticles.

References Cited

1. Huang, X.; Neretina, S.; El-Sayed, M. A., Gold nanorods: from synthesis and properties to biological and biomedical applications. *Adv Mater* 2009, *21*, 4880-4910.

2. Olson, T. Y.; Zhang, J. Z., Structural and optical properties and emerging applications of metal nanomaterials. *J Mater Sci Technol* 2008, *24* (4), 433-446.

3. Guihen, E.; Glennon, J. D., Nanoparticles in separation science - Recent developments. *Anal Lett* 2003, *36* (15), 3309-3336.

4. Turkevitch, J.; Stevenson, P. C.; Hillier, J., Nucleation and growth process in the synthesis of colloidal gold. *Discussions of the Faraday Society* 1951, *11*, 55.

5. Hu, M.; Chen, J.; Li, Z. Y.; Au, L.; Hartland, G. V.; Li, X.; Marquez, M.; Xia, Y., Gold nanostructures: engineering their plasmonic properties for biomedical applications. *Chemical Society Reviews* 2006, *35*, 1084-1094.

6. Gole, A.; Murphy, C. J., Seed-mediated synthesis of gold nanorods: Role of the size and nature of the seed. *Chem Mater* 2004, *16* (19), 3633-3640.

7. (a) Kelly, K. L.; Coronado, E.; Zhao, L. L.; Schatz, G. C., The optical properties of metal nanoparticles: The influence of size, shape, and dielectric environment. *J Phys Chem B* 2003, *107* (3), 668-677; (b) Mie, G., Articles on the optical characteristics of turbid tubes, especially colloidal metal solutions. *Ann Phys-Berlin* 1908, *25* (3), 377-445.

8. Ghosh, S. K.; Pal, T., Interparticle coupling effect on the surface plasmon resonance of gold nanoparticles: from theory to applications. *Chem Rev* 2007, *107* (11), 4797-4862.

9. Murphy, C. J.; Gole, A. M.; Hunyadi, S. E.; Stone, J. W.; Sisco, P. N.; Alkilany, A.; Kinard, B. E.; Hankins, P., Chemical sensing and imaging with metallic nanorods. *Chem Commun* 2008, (5), 544-557.

10. Murphy, C. J.; Sau, T. K.; Anand, M. G.; Orendorff, C. J.; Gao, J.; Gou, L.; Hunyadi, S. E.; Li, T., Anisotropic metal nanoparticles: synthesis, assembly, and optical applications. *J Phys Chem B* 2005, *109* (29), 13857-13870.

11. Treguer-Delapierre, M.; Majimel, J.; Mornet, S.; Duguet, E.; Ravaine, S., Synthesis of non-spherical gold nanoparticles. *Gold Bull* 2008, *41* (2), 195-207.

12. Xia, Y.; Xiong, Y. J.; Lim, B.; Skrabalak, S. E., Shape-Controlled Synthesis of Metal Nanocrystals: Simple Chemistry Meets Complex Physics? *Angew Chem Int Edit* 2009, *48* (1), 60-103.

13. (a) Sosa, I. O.; Noguez, C.; Barrera, R. G., Optical properties of metal nanoparticles with arbitrary shapes. *J Phys Chem B* 2003, *107* (26), 6269-6275; (b) Huang, Y.; Wang, W.; Liang, H.; Xu, H., Surfactant-promoted reductive synthesis of shape-controlled gold nanostructures. *Cryst Growth Des* 2009, *9* (2), 858-862.

14. Wang, C.; Ma, Z.; Wang, T.; Su, Z., Synthesis, assembly, and biofunctionalization of silica-coated gold nanorods for colorimetric sensing. *Adv Funct Mater* 2006, *16*, 1673-1678.

15. Nikoobakht, B.; El-Sayed, M. A., Preparation and growth mechanism of gold nanorods (NRs) using seed-mediated growth method. *Chem Mater* 2003, *15* (10), 1957-1962.

16. Perez-Juste, J.; Pastoriza-Santos, I.; Liz-Marzan, L. M.; Mulvaney, P., Gold nanorods: synthesis, characterization and applications. *Coordin Chem Rev* 2005, *249*, 1870-1901.

17. Gao, J. X.; Bender, C. M.; Murphy, C. J., Dependence of the gold nanorod aspect ratio on the nature of the directing surfactant in aqueous solution. *Langmuir* 2003, *19* (21), 9065-9070.

18. Sau, T. K.; Murphy, C. J., Room temperature, high-yield synthesis of multiple shapes of gold nanoparticles in aqueous solution. *J Am Chem Soc* 2004, *126* (28), 8648-8649.

19. Millstone, J. E.; Hurst, S. J.; Metraux, G. S.; Cutler, J. I.; Mirkin, C. A., Colloidal Gold and Silver Triangular Nanoprisms. *Small* 2009, *5* (6), 646-664.

20. Takezaki, M.; Kida, R.; Kato, Y.; Tominaga, T., Preparations of Triangular Gold Nanoplates by Chemical and Photoreduction Methods. *Chem Lett* 2009, *38* (11), 1022-1023.

21. Chu, H. C.; Kuo, C. H.; Huang, M. H., Thermal aqueous solution approach for the synthesis of triangular and hexagonal gold nanoplates with three different size ranges. *Inorg Chem* 2006, *45* (2), 808-813.

22. Caswell, K. K.; Wilson, J. N.; Bunz, U. H. F.; Murphy, C. J., Preferential end-to-end assembly of gold nanorods by biotin-streptavidin connectors. *J Am Chem Soc* 2003, *125* (46), 13914-13915.

23. Hu, X. G.; Cheng, W. L.; Wang, T.; Wang, E. K.; Dong, S. J., Well-ordered end-to-end linkage of gold nanorods. *Nanotechnology* 2005, *16* (10), 2164-2169.

24. Park, H. S.; Agarwal, A.; Kotov, N. A.; Lavrentovich, O. D., Controllable side-by-side and end-to-end assembly of au nanorods by lyotropic chromonic materials. *Langmuir* 2008, *24* (24), 13833-13837.

25. Joseph, S. T. S.; Ipe, B. I.; Pramod, P.; Thomas, K. G., Gold nanorods to nanochains: Mechanistic investigations on their longitudinal assembly using alpha,omega-alkanedithiols and interplasmon coupling. *J Phys Chem B* 2006, *110* (1), 150-157.

26. Schneider, H. J.; Schneider, U., The Host-Guest Chemistry of Resorcinarenes .1. *J Inclus Phenom Mol* 1994, *19* (1-4), 67-83.

27. Timmerman, P.; Verboom, W.; Reinhoudt, D. N., Resorcinarenes. *Tetrahedron* 1996, *52* (8), 2663-2704.

28. Bohmer, V., Calixarenes, Macrocycles with (Almost) Unlimited Possibilities. *Angewandte Chemie-International Edition in English* 1995, *34* (7), 713-745.

29. Kim, B.; Balasubramanian, R.; Perez-Segarra, W.; Wei, A.; Decker, B.; Mattay, J., Self-assembly of resorcinarene-stabilized gold nanoparticles: Influence of the macrocyclic headgroup. *Supramol Chem* 2005, *17* (1-2), 173-180.

30. Walker, D.; Gupta, V. K., Reversible end-to-end assembly of gold nanorods using a disulfide-modified polypeptide. *Nanotechnology* 2008, *19* (43).

31. Sharma, V.; Park, K.; Srinivasarao, M., Colloidal dispersion of gold nanorods: Historical background, optical properties, seed-mediated synthesis, shape separation and self-assembly. *Mat Sci Eng R* 2009, *65* (1-3), 1-38.

32. Sharma, V.; Park, K.; Srinivasarao, M., Shape separation of gold nanorods using centrifugation. *P Natl Acad Sci USA* 2009, *106* (13), 4981-4985.

33. Love, J. C.; Estroff, L. A.; Kriebel, J. K.; Nuzzo, R. G.; Whitesides, G. M., Self-assembled monolayers of thiolates on metals as a form of nanotechnology. *Chem Rev* 2005, *105* (4), 1103-1169.

34. Ulman, A., Formation and structure of self-assembled monolayers. *Chem Rev* 1996, *96* (4), 1533-1554.

35. Folkers, J. P.; Laibinis, P. E.; Whitesides, G. M., Self-assembled monolayers of alkanethiols on gold: comparisons of monolayers containing mixtures of short- and long-chain constituents with CH3 and CH2OH terminal groups. *Langmuir* 1992, *8* (5), 1330-1341.

36. Huang, W. L.; Chen, C. H.; Huang, M. H., Investigation of the growth process of gold nanoplates formed by thermal aqueous solution approach and the synthesis of ultra-small gold nanoplates. *J Phys Chem C* 2007, *111* (6), 2533-2538.